OsO_4 solution at 4°C for 2 h. After dehydration in an ethanol gradient (50–100% for 10 min each), samples were embedded in EPON812 at 60°C for 2 days. Ultrathin sections (80 nm) were stained using uranyl acetate and lead citrate. Sections were examined using an electron microscope (model JEM2000EX; JEOL, Tokyo, Japan) at 100 kV.

LDH cytotoxicity assay. Cytotoxicity assay was performed using a CytoTox 96 nonradioactive cytotoxicity assay kit (Promega, Madison, WI) in accordance with the instructions of the manufacturer. Briefly, after treating HUVECs at ~90% confluence in six-well plates with $C_{60}(OH)_{24}$ (1–100 μg/ml) for 24 h, culture medium was collected. Lactate dehydrogenase (LDH), a stable cytosolic enzyme released during cell lysis, was measured at 490-nm absorbance using a standard 96-well plate reader. Cytotoxicity was expressed relative to basal LDH release in untreated control cells.

Proliferation assay. Proliferation assay was performed using a Cell Counting-8 kit (Dojindo Laboratories, Kumamoto, Japan) according to the instructions of the manufacturer. Briefly, after treating HUVECs at ~30% confluence in 12-well plates with $C_{60}(OH)_{24}$ (1–100 μg/ml) for 24 h, water-soluble tetrazolium salt (WST-8) was added for 3 h and culture medium was collected. Conversion of WST-8 into formazan by living cells (active mitochondria) was measured using a standard 96-well plate reader at 450-nm absorbance. Total numbers of living cells were compared with untreated control samples.

Western blot analysis. Western blot analysis was performed as described previously (29). Proteins were obtained by homogenizing HUVECs with Triton X-based lysis buffer (1% Triton X-100, 20 mM Tris, pH 7.4, 150 mM NaCl, 1 mM EDTA, 1 mM EGTA, 2.5 mM sodium pyrophosphate, 1 mM β-glycerol phosphate, 1 mM Na_3VO_4, 1 μg/ml leupeptin, and 0.1% protease inhibitor mixture; Nacalai Tesque, Kyoto, Japan). Protein concentration was determined using the bicinchoninic acid method (Pierce, Rockford, IL). Equal amounts of proteins (15 μg) were separated by SDS-PAGE (7.5% and 14%) and transferred onto nitrocellulose membrane (Pall, Ann Arbor, MI). After being blocked with 3% BSA, membranes were incubated with primary antibody (1:1,000 dilution) at 4°C overnight and membrane-bound antibodies were visualized using horseradish peroxidase-conjugated secondary antibodies (1:10,000 dilution, 1 h) and the ECL system (Amersham Biosciences, Little Chalfont, UK). Experiments were performed three or more times, and equal loading of protein was ensured by measuring total actin expression.

Activity assay for 20S proteasome. Activity of the 20S proteasome was determined using the 20S proteasome assay kit (Calbiochem, San Diego, CA) according to the instructions of the manufacturer. Cells were lysed in Triton X-based lysis buffer as described above. The assay mixture contained 178 μl of reaction buffer (25 mM HEPES and 0.5 mM EDTA, pH 7.6), 10 μl of substrate [10 μM Suc-Leu-Val-Tyr-7-amino-4-methylcoumarin (AMC)], 2 μl of SDS (0.03%), and 10 μl of cell lysate (10 μg of protein). After incubation for 30 min at 37°C, the fluorescence of liberated AMC was measured using excitation and emission wavelengths at 340 and 450 nm, respectively.

Microarray analysis. Total RNA was isolated from HUVECs treated with or without $C_{60}(OH)_{24}$ (100 μg/ml, 24 h) using an RNeasy Kit (Qiagen, Valencia, CA) according to the instructions of the manufacturer. Only samples with A260/A280 between 1.7 and 2.2 (measured in 10 mM Tris·HCl, pH 7.6) were considered suitable for use. Hybridization samples were prepared according to the *GeneChip Expression Analysis Technical Manual* (701021, Rev. 5, section 2,

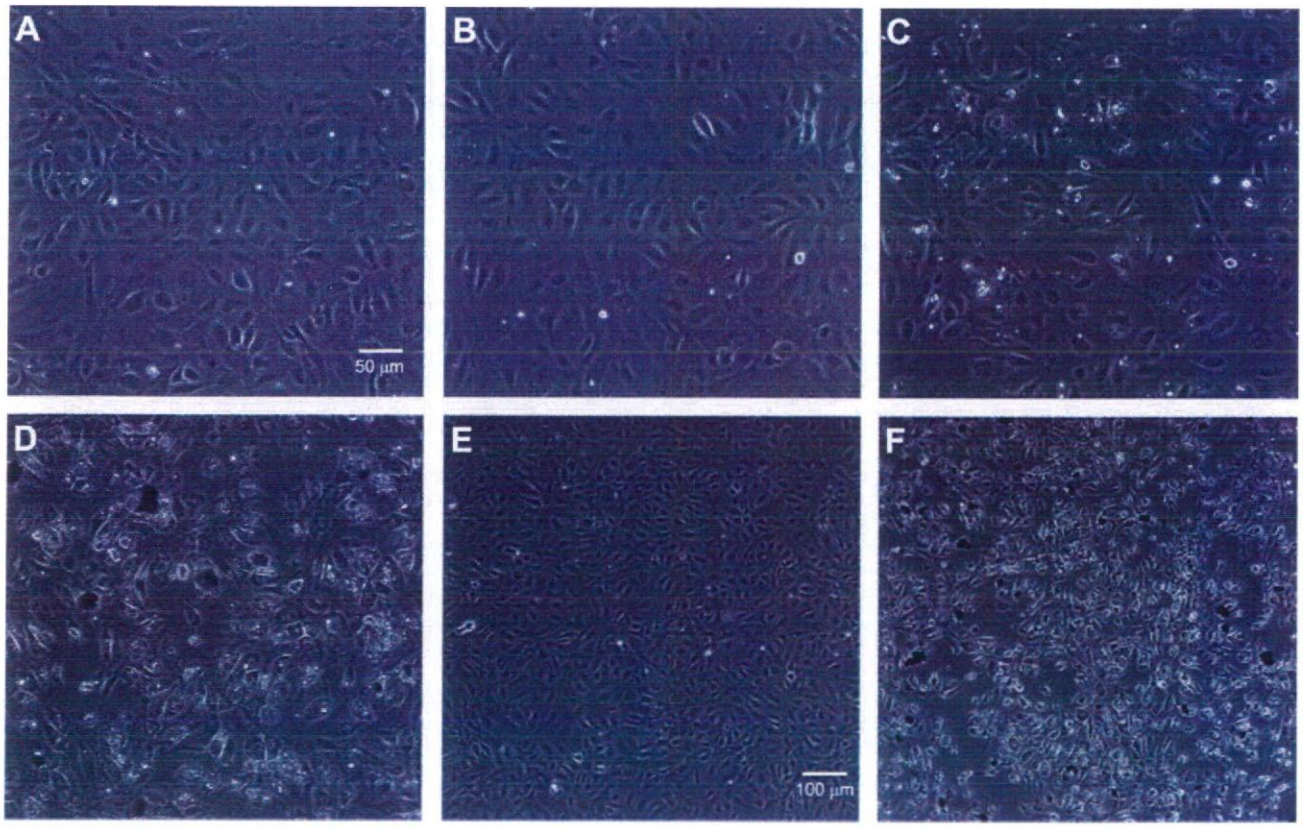

Fig. 1. Representative photomicrographs of human umbilical vein endothelial cells (HUVECs) treated with hydroxyl fullerene [$C_{60}(OH)_{24}$]. HUVECs at ~90% confluence were treated with $C_{60}(OH)_{24}$ (*A* and *E*: 0 μg/ml; *B*: 1 μg/ml; *C*: 10 μg/ml; *D* and *F*: 100 μg/ml) for 24 h. Scale bars, 50 μm (*A–D*) and 100 μm (*E* and *F*).

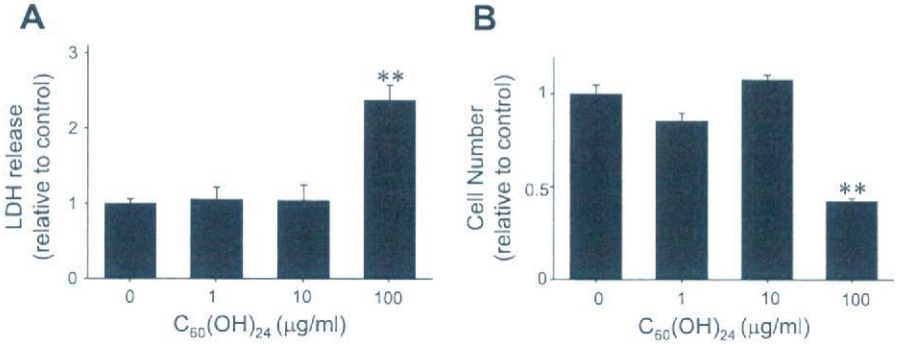

Fig. 2. Fullerene-induced cytotoxic injury in HUVECs. HUVECs at ~90% confluence were treated with $C_{60}(OH)_{24}$ (1–100 μg/ml for 24 h). Culture medium was then collected. *A*: lactate dehydrogenase (LDH) released into the supernatant was measured using a commercially available kit. Cytotoxicity was expressed relative to basal LDH release in controls (n = 4–11). *B*: living cell number was calculated using water-soluble tetrazolium salt (WST-8). n = 3; $^{**}P < 0.01$ vs. controls.

"Eukaryotic Sample and Array Processing," chapt. 1, "Eukaryotic Target Preparation"; http://www.affymetrix.com/support/technical/manuals.affx). Total RNA (2 μg) was amplified for each sample. Next, cRNA (30 μg) was fragmented in 40 μl of 1× fragmentation buffer. Hybridization cocktails were made as described in the *GeneChip Expression Analysis Technical Manual* (701021, Rev. 5, section 2, chapt. 2, "Eukaryotic Target Hybridization") and hybridized to human genome U133 plus2.0 chips at 60 rpm and 45°C for 16 h using the Hybridization Oven 640 110 V (no. 800138; Affymetrix, Santa Clara, CA). Human genome U133 plus2.0 chips (Affymetrix) comprise 54,000 probe sets and provide comprehensive coverage of the transcribed human genome on a single array to analyze expression levels of >47,000 transcripts and variants, including 38,500 well-characterized human genes plus ~6,500 new genes. GeneChips were stained with streptavidin-phycoerythrin using a Fluidics Station 450 (00-0079; Affymetrix). After being washed extensively, GeneChips were scanned using a GeneChip Scanner 3000 (00-0074; Affymetrix). Data were analyzed using GeneChip Operating Software version 1.1 (no. 690036; Affymetrix) according to GeneChip Expression Analysis Data Analysis Fundamentals (chapt. 4, "First-Order Data Analysis and Data Quality Assessment"; and chapt. 5, "Statistical Algorithms Reference"; http://www.affymetrix.com/support/technical/manuals.

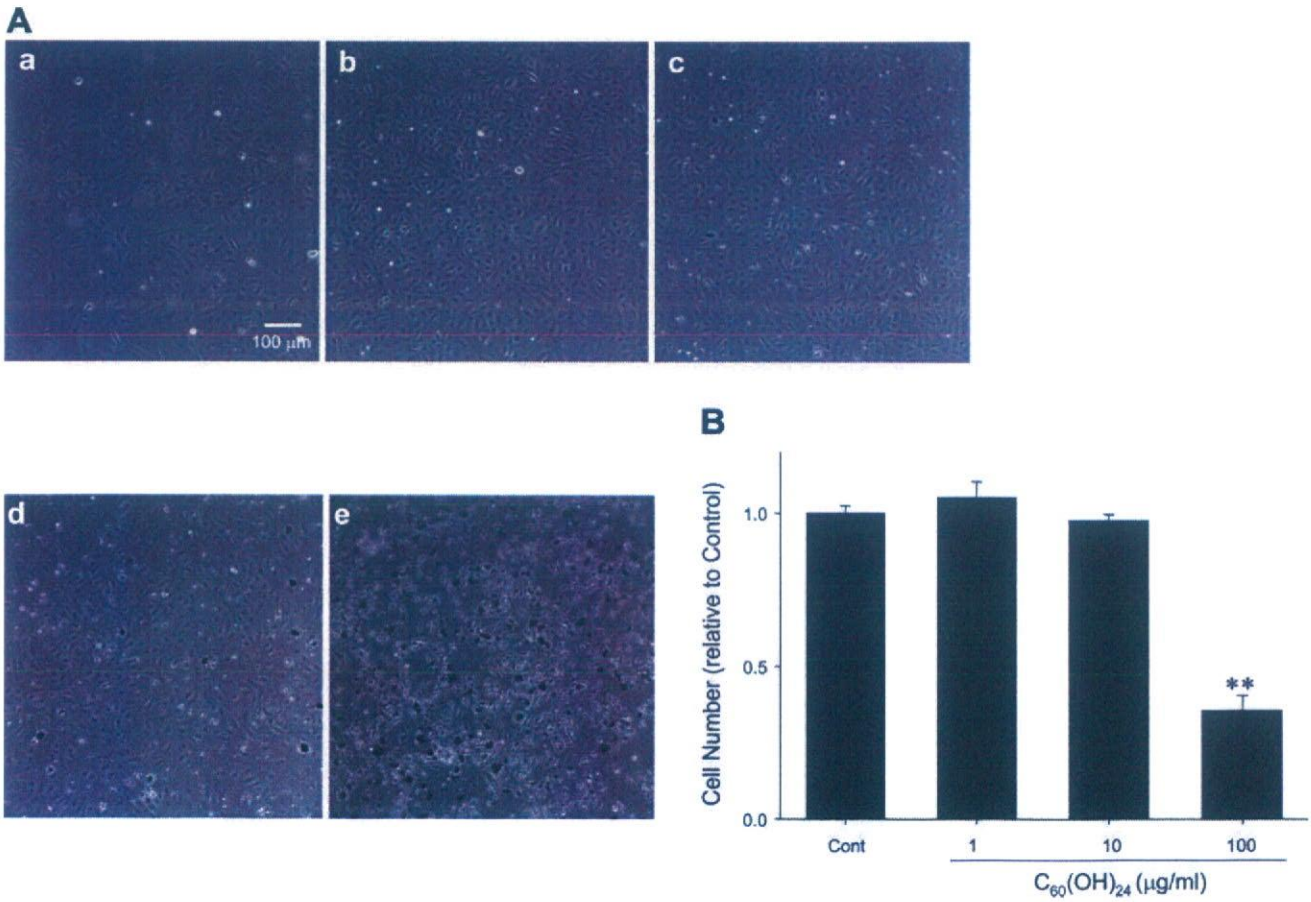

Fig. 3. Fullerene-inhibited cell growth in HUVECs. HUVECs at ~30% confluence were treated with $C_{60}(OH)_{24}$ (1–100 μg/ml) for 24 h. *A*: representative photomicrographs are shown (*a*: Start; *b*: 0 μg/ml; *c*: 1 μg/ml; *d*: 10 μg/ml; and *e*: 100 μg/ml; all for 24 h). Scale bar, 100 μm. *B*: total number of living cells was counted using WST-8. Results are shown relative to controls. n = 6; $^{**}P < 0.01$ vs. controls.

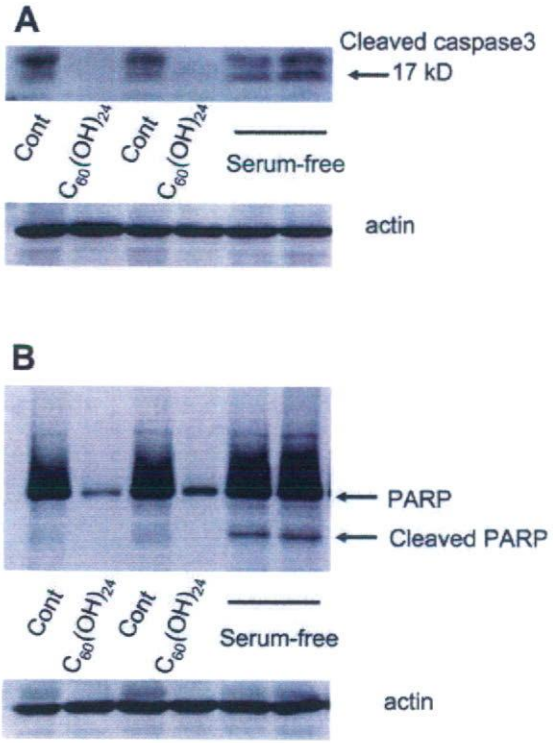

Fig. 4. Fullerene does not induce apoptosis in HUVECs. After HUVECs at ~90% confluence were treated with 100 μg/ml $C_{60}(OH)_{24}$ for 24 h, total cell lysates were harvested. Cleaved caspase-3 (17 kDa; *A*) and poly(ADP-ribose) polymerase (PARP; *B*) expression were determined using Western blot analysis. Equal protein loading was confirmed using total actin antibody.

affx). To allow comparison, all chips were scaled to a target intensity of 500 on the basis of all probe sets on each chip. Comparison of GeneChip array data was obtained using custom analysis services (Kurabo Industries, Osaka, Japan). Kurabo Industries is the authorized service provider for Affymetrix Japan (Tokyo, Japan). Genes that were significantly upregulated (top 100 genes; see Supplemental Table 1; http://ajpcell.physiology.org/cgi/content/full/00481.2005/DC1) or downregulated (top 100 genes; Supplemental Table 2) in two independent experiments are summarized. Microarray data were deposited in the National Center for Biotechnology Information's Gene Expression Omnibus (GenBank accession no. GSE3364).

Statistical analysis. Data are means ± SE. Statistical evaluations were performed using an unpaired Student's *t*-test. Values of $P < 0.05$ were considered statistically significant.

RESULTS

Fullerene induces cytotoxic morphological changes in HUVECs. To examine the direct effects on vascular ECs, cultured HUVECs were treated with $C_{60}(OH)_{24}$ for 24 h. Fullerenes (1–100 μg/ml) induced cytotoxic morphological changes in HUVECs such as vacuole formation in the cytosol and decreased cell density in a dose-dependent manner (Fig. 1, *A–D*). Figure 1, *E* (Control) and *F* [100 μg/ml $C_{60}(OH)_{24}$], represent low-magnification pictures, and cell density was clearly decreased after treatment with fullerene.

Fullerene increases release of LDH from HUVECs. To assess EC injury by fullerene quantitatively, we examined the effects of fullerenes on endothelial LDH release, a marker of cell death and injury of the plasma membrane. Although 10 μg/ml $C_{60}(OH)_{24}$ showed slight cytotoxic morphological changes (Fig. 1*C*), only the maximal concentration of $C_{60}(OH)_{24}$ (100 μg/ml, 24 h, $n = 8$) significantly increased LDH release into culture medium (Fig. 2*A*) (LDH increased 2.4 ± 0.2-fold vs. controls, $n = 11$; $P < 0.01$). To further explore the degree of cell injury after fullerene treatment, we calculated the living cell number using WST-8. A maximal dose of 100 μg/ml $C_{60}(OH)_{24}$ killed 58.0 ± 1.7% of cells ($n = 3$; $P < 0.01$ vs. controls) (Fig. 2*B*).

Fullerene has antiproliferative effects on HUVECs. To examine the effects of fullerene on cell growth, HUVECs at ~30% confluence were treated with $C_{60}(OH)_{24}$ (1–100 μg/ml) for 24 h and then the total number of living cells was measured using WST-8. HUVEC growth was inhibited by $C_{60}(OH)_{24}$ in a dose-dependent manner (Fig. 3*A*). Quantitative analysis (Fig. 3*B*) revealed that only the maximal concentration of 100 μg/ml $C_{60}(OH)_{24}$ significantly inhibited cell growth (64.2 ± 4.7%, $n = 6$; $P < 0.01$ vs. controls).

Fullerene does not induce apoptosis in HUVECs. We next examined whether fullerene induces apoptosis in vascular ECs. Serum starvation but not a maximal dose of $C_{60}(OH)_{24}$ (100 μg/ml, 24 h) induced cleavage of caspase-3 (17 kDa) and PARP (Fig. 4), which are markers for the activation of the apoptotic cascade (5, 20). This suggests that fullerene does not induce apoptosis in HUVECs. Notably, protein bands for both

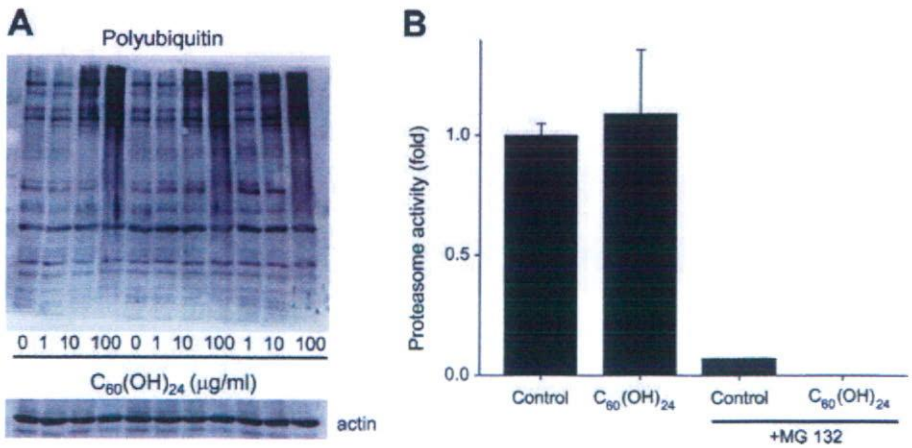

Fig. 5. Fullerene treatment induces polyubiquitination in HUVECs. After HUVECs at ~90% confluence were treated with $C_{60}(OH)_{24}$ (1–100 μg/ml) for 24 h, total cell lysates were harvested. *A*: accumulation of polyubiquitin was determined using Western blot analysis. Equal protein loading was confirmed using total actin antibody ($n = 8$). *B*: activity of the 20S proteasome was determined using a commercially available kit. Activity of 20S proteasomes was measured on the basis of fluorescence of liberated amino-4-methylcoumarin (AMC) using excitation and emission wavelengths at 340 and 450 nm. Results shown are relative to controls ($n = 3$).

caspase-3 and PARP were weak in $C_{60}(OH)_{24}$-treated samples. This finding is consistent with fullerene-treated samples in other immunoblot analysis experiments. We speculate that this phenomenon is due to protein degeneration by fullerene.

Fullerene induces accumulation of polyubiquitinated proteins in HUVECs. Because activation of the ubiquitin-proteasome system represents another death pathway, protein polyubiquitination by fullerene was examined. $C_{60}(OH)_{24}$ (1–100 μg/ml, 24 h, $n = 8$) induced protein polyubiquitination in a dose-dependent manner (Fig. 5*A*). Proteasome activity assay showed that 100 μg/ml $C_{60}(OH)_{24}$ (24 h) did not directly modify it (Fig. 5*B*) (1.09 ± 0.27-fold increase vs. controls; $n = 3$). Proteasome activity in cell lysates was suppressed almost completely by a proteasome inhibitor, MG132 (1 μM).

Ultrastructural features of HUVECs: fullerene facilitates autophagic cell death. We next performed ultrastructural analysis using transmission electron microscopy. The cytoplasm of untreated HUVECs (control) (Fig. 6*A*) contained small vesicles. In vascular smooth muscle cells, the formation of small vesicles reportedly occurs under normal physiological conditions to remove abnormal proteins and cytoplasmic macromolecules (15). Treatment of HUVECs with the maximal dose of $C_{60}(OH)_{24}$ (100 μg/ml, 24 h) caused extensive vacuolization and internalization of fullerene (Fig. 6*B*). Fullerene aggregates were observed primarily within autophagosome-like vesicles (Fig. 6, *C* and *D*). To show that vesicles represented autophagosomes, Western blot analysis was performed to detect LC3 II because conversion of LC3 I (cytosolic isoform) to LC3 II (membrane-bound form) are frequently used markers for autophagosomes (9, 32). Figure 7 clearly shows that 100 μg/ml $C_{60}(OH)_{24}$ (24 h) increased levels of the LC3 II isoform ($n = 4$).

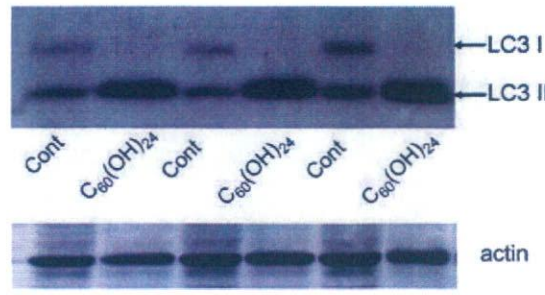

Fig. 7. Fullerene induced the formation of autophagosomes in HUVECs. After HUVECs at ~90% confluence were treated with 100 μg/ml $C_{60}(OH)_{24}$ for 24 h, total cell lysates were harvested. Autophagosomes were detected using Western blot analysis with light chain (LC)3 antibody ($n = 4$). *Top band* represents cytosolic LC3 I, and *bottom band* represents membrane-bound LC3 II, a typical marker for autophagosomes. Equal protein loading was confirmed using total actin antibody.

Chronic effects of low-dose fullerene on EC toxicity. We examined the chronic effects of low concentrations of $C_{60}(OH)_{24}$ (1–10 μg/ml, up to 10 days) on EC toxicity. During this time, cells were subcultured three times (*passages 3–6*). Media containing fullerene were changed every 2 days. Chronic treatment with 1 μg/ml $C_{60}(OH)_{24}$ for 10 days had no significant effects on EC toxicity (data not shown). Figure 8 shows the morphological features of HUVECs treated without (control) or with 10 μg/ml $C_{60}(OH)_{24}$. Fullerene was treated soon after splitting cells from *passages 3* to *4*. On *day 2*, both control and fullerene-treated cells reached subconfluence, but fullerene-treated cells showed clear morphological changes such as cytosolic vacuole formation and spindlelike cell shape.

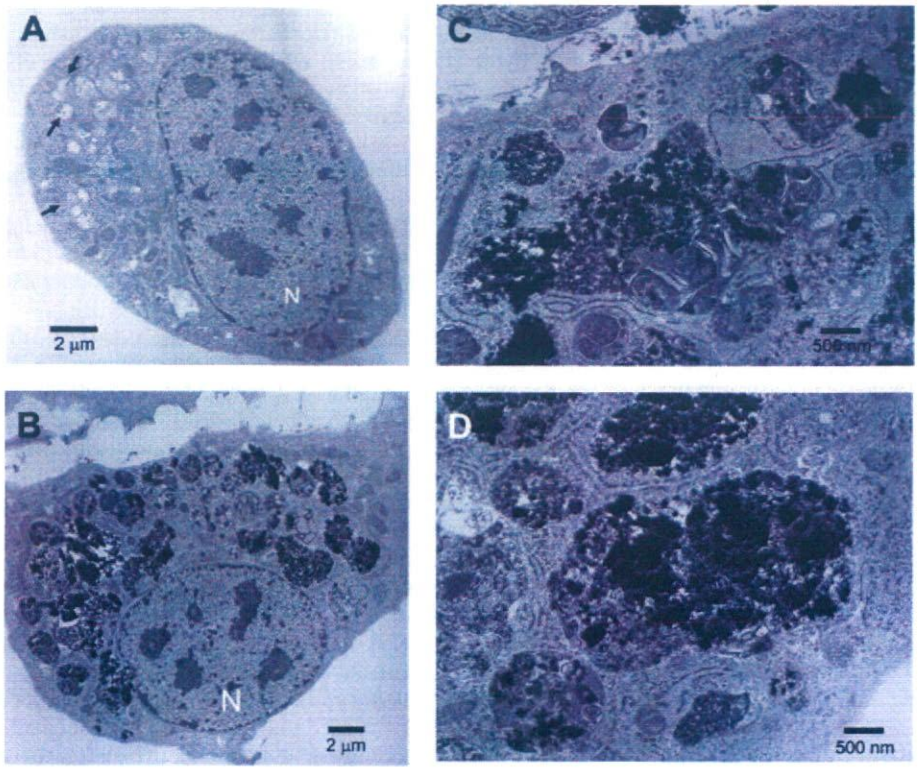

Fig. 6. Ultrastructural features of HUVECs treated with $C_{60}(OH)_{24}$. HUVECs were treated without (*A*; control) or with 100 μg/ml $C_{60}(OH)_{24}$ (*B–D*) for 24 h. N, nucleus. Arrows indicate vacuoles with phagocytotic function. Scale bars, 2 μm (*A* and *B*) and 500 nm (*C* and *D*).

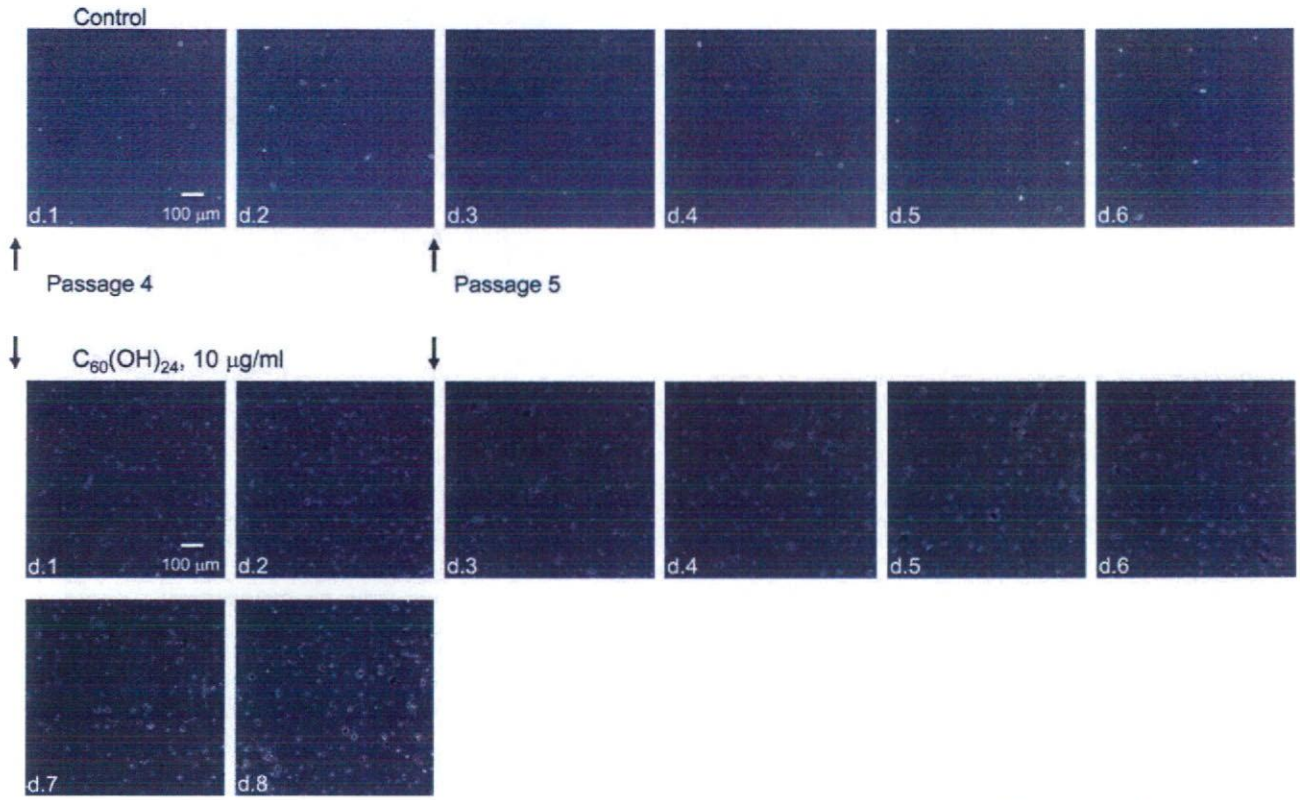

Fig. 8. Chronic effects of low-dose fullerene on HUVECs. HUVECs were treated without (Control) or with 10 μg/ml $C_{60}(OH)_{24}$ for 8 days. Cells from *passages 4* and *5* were used. Treatment was started soon after splitting cells from *passages 3* and *4*. Culture media containing fullerene were changed every 2 days. Representative morphological features are shown. Scale bar, 100 μm. Arrows indicate time of splitting.

After the second passage, control cells reached confluence within 4 days. In contrast, the attachment of cells (*day 3*) was bad in fullerene-treated groups and cell growth speed was slow. On *day 8*, fullerene-treated cells reached confluence, but the shapes of the cells were bad (spindlelike) and vacuole formation was commonly observed, suggesting the possibility that fullerene-resistant types of cells survived and increased.

Microarray analysis. Finally, microarray analysis was performed using total RNA from HUVECs treated with the maximal dose of $C_{60}(OH)_{24}$ (100 μg/ml, 24 h). Results from 2 independent samples are summarized in Supplemental Tables 1 and 2. Of note, although these were not top 100 genes, several genes related to the ubiquitin-proteasome system were significantly upregulated by fullerene [HECT (a COOH-terminal catalytic homologous to E6-AP-COOH terminus domain), C2, and WW domain containing E3 ubiquitin protein ligase 2 (ratio, 2.3 to 1), ubiquitin-specific protease 31 (ratio, 1.7 to 1), ubiquitin-specific protease 32 (ratio, 1.7 to 1), and ubiquitin-conjugating enzyme E2 (ratio, 1.5 to 1)].

DISCUSSION

The major findings of the present study are that water-soluble fullerene directly affects vascular ECs to cause cytotoxic injury or cell death and inhibition of cell growth. To the best of our knowledge, this study provides the first demonstration of the direct effects of water-soluble fullerene on vascular endothelium. In other human cells, including dermal fibroblasts, liver carcinoma cells (HepG2), neuronal astrocytes, and T-lymphocytes (Jurkat cells), recent reports have noted that water-soluble fullerene shows cytotoxic effects, presumably via production of reactive oxygen species (22, 24). Notably, several types of water-soluble fullerene derivatives are available [e.g., hydroxyl fullerene used herein, dendritic C_{60} monoadduct (22), malonic acid C_{60} (22) and nano-C_{60} (24) (basically pristine C_{60})], and cytotoxicity to cells varies depending on the fullerene subtype used, presumably because of surfactant chemistry, including a balance between hydrophobicity and hydrophilicity (3).

Some novel mechanistic insights of this study are that fullerene causes EC injury or cell death by increasing the accumulation of polyubiquitinated proteins in the cytosol and facilitating excessive autophagic cell death. EC injury and death are closely related to the initiation of atherosclerosis (14, 23). Furthermore, through nitric oxide production, ECs offer important protective functions against ischemic heart disease, including myocardial infarction, by inhibiting platelet aggregation (16) and lowering blood pressure (27). We thus propose that exposure to nanomaterials is a potential risk for cardiovascular disease, including atherosclerosis and ischemic heart disease. However, because quantitatively significant EC toxicity from water-soluble fullerene was observed only at high dosage, further validations (particularly in vivo) are needed.

We recently found that carbon black (CB), a chemically inert carbon nanoparticle present in diesel exhaust particles

(13), shows endothelial cytotoxicity by mechanisms different from those of fullerene (31). Specifically, microarray analysis revealed that CB stimulated the induction of several proinflammatory mediators, including E-selectin, ICAM-I, IL-8, heme oxygenase-1, and prostaglandin endoperoxide synthase 2. However, such effects were not observed in fullerene-stimulated ECs. Furthermore, CB did not cause accumulation of polyubiquitinated proteins in ECs. Although the underlying mechanisms remain unclear, our findings indicate that the results reported herein could be specific to fullerene. Another report (21) examined the effects of several nanomaterials, including metals (TiO_2, SiO_2, Co, Ni, polyvinyl chloride), on endothelial toxicity. The report showed that only Co^{2+} particles possessed cytotoxic effects on ECs, supporting the concept that cytotoxicity varies among different nanoparticles.

Several pathways lead to cell death (6). Two major types of programmed cell death have been distinguished: the caspase-mediated process of apoptosis and the caspase-independent process involving autophagy.

In the present study, we found that exposure to fullerene did not induce cleavage of caspase-3 or PARP, which are the hallmarks of apoptosis (5, 20). Furthermore, no clear chromatin condensation was apparent in the nuclei (Fig. 6*B*). The present results thus indicate that the induction of apoptosis does not seem to be responsible for fullerene-induced cell death and/or injury.

Conversely, fullerene markedly increased the accumulation of polyubiquitinated proteins (Fig. 5*A*). Normally, under physiological conditions, cells degrade ubiquitinated proteins using 20S proteasomes. Fullerene does not seem to modify proteasome activity directly (Fig. 5*B*). Ultrastructural analysis revealed the excess formation of phagosome-like vesicles in the cytosol (Fig. 6*B*). Vesicles have been determined to be autophagosomes on the basis of Western blot analysis using specific marker LC3 II (9, 32) (Fig. 7). Similarly, the formation of phagosomes was observed after treating alveolar macrophages with single-wall and multiwall carbon nanotubes (8). Autophagy (type II programmed death) is known to be an alternative pathway to exclude unnecessary proteins and cellular organelles. We thus propose that accumulation of ubiquitinated proteins and abnormal activation of an autophagic death pathway could be responsible at least for cell death or injury caused by water-soluble fullerene.

EC injury and/or death appears to represent a primary mechanism for the initiation of atherosclerosis (14, 23). Injury and/or denudation of ECs trigger the attachment of leukocytes to the subendothelial region and promote transendothelial migration of cells, allowing the initiation of atherosclerosis. EC injury also leads to the loss of beneficial functions, including antithrombogenic and blood pressure-lowering functions via nitric oxide, which leads to the progression of ischemic heart disease, including myocardial infarction. In addition to cell death and injury, fullerene also inhibited EC growth. Impairment of EC growth may be related to impairment of angiogenesis. Because angiogenesis is crucial to the maintenance of vascular integrity by forming collateral vessels in response to tissue ischemia (11), fullerene inhibition of EC growth may be related to the progression of ischemic heart disease. Collectively, the present findings support the concept that exposure to fullerene could be a risk for atherosclerosis and ischemic heart disease.

The present study used 1–100 μg/ml fullerene concentrations for in vitro experiments. The pathophysiological concentrations of fullerene are barely known. In addition to engineered nanomaterials, traffic-derived nanoparticles are known to represent a risk for cardiovascular disorders, including atherosclerosis and ischemic heart disease (2, 4). The maximal concentration of particulate matter <2.5 μm in Chongqing, one of the biggest cities in China, was ~700 $\mu g/m^3$ (daily average) (26), indicating that an individual could inhale ~10,000 μg of particulate matter during the course of 24 h there. This value is equivalent to ~1 μg/ml when the extracellular fluid volume is 12 L in a 60-kg person. The fullerene dosage used in this study was up to 100-fold higher than this level.

The kinetics of water-soluble fullerene in vivo have not yet been completely determined. Normally, inhaled microparticles are cleaned off by alveolar macrophages via phagocytosis. However, this is not applicable to nanoparticles (2, 19), which appear to translocate to extrapulmonary sites via blood and lymph and thus reach other tissues (19). Using radiolabeled water-soluble fullerene administered intravenously to rats, Yamago et al. (28) demonstrated that most fullerenes moved rapidly to the liver (within 1 h) and then were distributed to various other tissues, including spleen, lung, kidney, heart, and brain. Extraction seems slow, and >90% was retained in the body 1 wk later, raising concern about chronic toxic effects. Although we could not clearly observe EC cytotoxicity after acute treatment with low-dose fullerene (10 μg/ml, 24 h), treatment for 8 days seems to enhance toxicity (Fig. 8). The effects of chronic exposure to low-dose fullerene in vivo need to be examined, particularly with regard to the cardiovascular system.

In summary, in the present study, we examined the direct effects of water-soluble fullerene on vascular endothelial cells to explore the potential toxicity of fullerene in humans, especially regarding the cardiovascular systems. We found that fullerene causes cytotoxic injury or cell death in vascular ECs, indicating that exposure to fullerene could represent a risk for atherosclerosis and ischemic heart disease. Because cytotoxicity by water-soluble fullerene occurs only at high doses, further validation experiments using blood vessels and animal models are warranted.

ACKNOWLEDGMENTS

We are grateful to Dr. T. Yoshimori (National Institute of Genetics, Mishima, Japan) for providing LC3 antibody.

GRANTS

This study was supported by Health and Labor Sciences Research Grant for Research on Risk of Chemical Substance Grant H17-Chemistry-008 (to N. Iwai) and Grant-in-Aid for Scientific Research Grant 17790176 (to H. Yamawaki) from the Ministry of Education, Culture, Sports, Science, and Technology, Japan.

REFERENCES

1. **Åkerman ME, Chan WCW, Laakkonen P, Bhatia SN, and Ruoslahti E.** Nanocrystal targeting in vivo. *Proc Natl Acad Sci USA* 99: 12617–12621, 2002.
2. **Borm PJA and Kreyling W.** Toxicological hazards of inhaled nanoparticles: potential implications for drug delivery. *J Nanosci Nanotechnol* 4: 521–531, 2004.
3. **Bosi S, Feruglio L, Da Ros T, Spalluto G, Gregoretti B, Terdoslavich M, Decorti G, Passamonti S, Moro S, and Prato M.** Hemolytic effects of water-soluble fullerene derivatives. *J Med Chem* 47: 6711–6715, 2004.

4. **Brook RD, Franklin B, Cascio W, Hong Y, Howard G, Lipsett M, Luepker R, Mittleman M, Samet J, Smith SC Jr, and Tager I.** Air pollution and cardiovascular disease: a statement for healthcare professionals from the Expert Panel on Population and Prevention Science of the American Heart Association. *Circulation* 109: 2655–2671, 2004.
5. **Budihardjo I, Oliver H, Lutter M, Luo X, and Wang X.** Biochemical pathways of caspase activation during apoptosis. *Annu Rev Cell Dev Biol* 15: 269–290, 1999.
6. **Clarke PG.** Developmental cell death: morphological diversity and multiple mechanisms. *Anat Embryol (Berl)* 181: 195–213, 1990.
7. **Colvin VL.** The potential environmental impact of engineered nanomaterials. *Nat Biotechnol* 21: 1166–1170, 2003.
8. **Jia G, Wang H, Yan L, Wang X, Pei R, Yan T, Zhao Y, and Guo X.** Cytotoxicity of carbon nanomaterials: single-wall nanotube, multi-wall nanotube, and fullerene. *Environ Sci Technol* 39: 1378–1383, 2005.
9. **Kabeya Y, Mizushima N, Ueno T, Yamamoto A, Kirisako T, Noda T, Kominami E, Ohsumi Y, and Yoshimori T.** LC3, a mammalian homologue of yeast Apg8p, is localized in autophagosome membranes after processing. *EMBO J* 19: 5720–5728, 2000.
10. **Katsouyanni K, Touloumi G, Samoli E, Gryparis A, Le Tertre A, Monopolis Y, Rossi G, Zmirou D, Ballester F, Boumghar A, Anderson HR, Wojtyniak B, Paldy A, Braunstein R, Pekkanen J, Schindler C, and Schwartz J.** Confounding and effect modification in the short-term effects of ambient particles on total mortality: results from 29 European cities within the APHEA2 project. *Epidemiology* 12: 521–531, 2001.
11. **Kondo T, Kobayashi K, and Murohara T.** Nitric oxide signaling during myocardial angiogenesis. *Mol Cell Biochem* 264: 25–34, 2004.
12. **Kreuter J.** Nanoparticulate systems for brain delivery of drugs. *Adv Drug Deliv Rev* 47: 65–81, 2001.
13. **Lam CW, James JT, McCluskey R, and Hunter RL.** Pulmonary toxicity of single-wall carbon nanotubes in mice 7 and 90 days after intratracheal instillation. *Toxicol Sci* 77: 126–134, 2004.
14. **Libby P.** Inflammation in atherosclerosis. *Nature* 420: 868–874, 2002.
15. **Martinet W, De Bie M, Schrijvers DM, De Meyer GR, Herman AG, and Kockx MM.** 7-Ketocholesterol induces protein ubiquitination, myelin figure formation, and light chain 3 processing in vascular smooth muscle cells. *Arterioscler Thromb Vasc Biol* 24: 2296–2301, 2004.
16. **Moncada S, Palmer RM, and Higgs EA.** Nitric oxide: physiology pathophysiology, and pharmacology. *Pharmacol Rev* 43: 109–142, 1991.
17. **Nemmar A, Hoet PH, Vanquickenborne B, Dinsdale D, Thomeer M, Hoylaerts MF, Vanbilloen H, Mortelmans L, and Nemery B.** Passage of inhaled particles into the blood circulation in humans. *Circulation* 105: 411–414, 2002.
18. **Nemmar A, Hoylaerts MF, Hoet PH, and Nemery B.** Possible mechanisms of the cardiovascular effects of inhaled particles: systemic translocation and prothrombotic effects. *Toxicol Lett* 149: 243–253, 2004.
19. **Oberdorster G, Oberdorster E, and Oberdorster J.** Nanotoxicology: an emerging discipline evolving from studies of ultrafine particles. *Environ Health Perspect* 113: 823–839, 2005.
20. **Patel T, Gores GJ, and Kaufmann SH.** The role of proteases during apoptosis. *FASEB J* 10: 587–597, 1996.
21. **Peters K, Unger RE, Kirkpatrick CJ, Gatti AM, and Monari E.** Effects of nano-scaled particles on endothelial cell function in vitro: studies on viability, proliferation and inflammation. *J Mater Sci Mater Med* 15: 321–325, 2004.
22. **Rancan F, Rosan S, Boehm F, Cantrell A, Brellreich M, Schoenberger H, Hirsch A, and Moussa F.** Cytotoxicity and photocytotoxicity of a dendritic C_{60} mono-adduct and a malonic acid C_{60} tris-adduct on Jurkat cells. *J Photochem Photobiol B* 67: 157–162, 2002.
23. **Ross R.** Atherosclerosis: an inflammatory disease. *N Engl J Med* 340: 115–126, 1999.
24. **Sayes CM, Gobin AM, Ausman KD, Mendez J, West JL, and Colvin VL.** Nano-C_{60} cytotoxicity is due to lipid peroxidation. *Biomaterials* 26: 7587–7595, 2005.
25. **Seaton A and Donaldson K.** Nanoscience, nanotoxicology, and the need to think small. *Lancet* 365: 923–924, 2005.
26. **Venners SA, Wang B, Xu Z, Schlatter Y, Wang L, and Xu X.** Particulate matter, sulfur dioxide, and daily mortality in Chongqing, China. *Environ Health Perspect* 111: 562–567, 2003.
27. **Wilkinson IB, Franklin SS, and Cockcroft JR.** Nitric oxide and the regulation of large artery stiffness: from physiology to pharmacology. *Hypertension* 44: 112–116, 2004.
28. **Yamago S, Tokuyama H, Nakamura E, Kikuchi K, Kananishi S, Sueki K, Nakahara H, Enomoto S, and Ambe F.** In vivo biological behavior of a water-miscible fullerene: [^{14}C] labeling, absorption, distribution, excretion and acute toxicity. *Chem Biol* 2: 385–389, 1995.
29. **Yamawaki H, Lehoux S, and Berk BC.** Chronic physiological shear stress inhibits tumor necrosis factor-induced proinflammatory responses in rabbit aorta perfused ex vivo. *Circulation* 108: 1619–1625, 2003.
30. **Yamawaki H, Pan S, Lee RT, and Berk BC.** Fluid shear stress inhibits vascular inflammation by decreasing thioredoxin-interacting protein in endothelial cells. *J Clin Invest* 115: 733–738, 2005.
31. **Yamawaki H and Iwai N.** Mechanisms underlying nano-sized air pollution-mediated progression of atherosclerosis: carbon black causes cytotoxic injury/inflammation and inhibits cell growth in vascular endothelial cells. *Circ J* 70: 129–140, 2006.
32. **Yoshimori T.** Autophagy: a regulated bulk degradation process inside cells. *Biochem Biophys Res Commun* 313: 453–458, 2004.

[Environmental Health and Preventive Medicine 11, 292–297, November 2006]

Original Article

Genotoxicity in Cell Lines Induced by Chronic Exposure to Water-Soluble Fullerenes Using Micronucleus Test

Yasuharu NIWA[1] and Naoharu IWAI[1]

[1]*Department of Epidemiology, Research Institute, National Cardiovascular Center, Osaka, Japan*

Abstract

Objectives: Nanomaterials have numerous potential benefits for society, but the effects of nanomaterials on human health are poorly understood. In this study, we aim to determine the genotoxic effects of chronic exposure to nanomaterials in various cell lines.

Methods: Chinese hamster ovary (CHO) cells, human epidermoid-like carcinoma (Hela) cells and human embryonic kidney 293 (HEK293) cells were treated with the water-soluble fullerene $C_{60}(OH)_{24}$ for 33–80 days. Cell proliferation, cytotoxic analysis and micronucleus tests were performed.

Results: When treated with $C_{60}(OH)_{24}$ (0, 10, 100, or 1000 pg/ml) for 33 days, both the HEK293 and Hela cells showed increased cell proliferation, but cellular lactate dehydrogenase (LDH) activity was not affected. After long-term exposure (80 days) to $C_{60}(OH)_{24}$ (0, 10, 100, or 1000 pg/ml), the CHO, Hela and HEK293 cells showed increased genotoxicity on the micronucleus test.

Conclusion: This study suggests that nanomaterials, such as $C_{60}(OH)_{24}$, have genotoxic effects.

Key words: water-soluble fullerene, genotoxicity, micronucleus test

Introduction

Environmental health studies have focused on the relationship between health outcome and ambient levels of PM10 and PM2.5, which are particles having aerodynamic diameters <10 and 2.5 μm, respectively. Recently, however, epidemiological studies have begun focusing on ultrafine particles (UFPs) having a diameter of <100 nm, which are abundant but account for a small proportion of total particle mass. UFPs are important with regard to adverse health effects due to their high alveolar deposition fraction (1–3).

Biomedical applications under development include targeted drug delivery systems for brain and tumor tissues, as well as intravascular nanosensor and nanorobotic devices for imaging and diagnosis. However, the potential adverse effects or humeral response following the introduction of nanomaterials into an organism remain unknown (4–6). After inhaled nanomaterials are deposited in the respiratory tract, their small size allows cellular uptake and transcytosis into the vascular and lymphatic systems.

Received Jun. 12, 2006/Accepted Aug. 30, 2006
Reprint requests to: Yasuharu NIWA, PhD
Department of Epidemiology, Research Institute, National Cardiovascular Center, Suita, Osaka 565-8565, Japan
TEL: +81(6)6833-5012, FAX: +81(6)6835-2088
E-mail: yniwa@ri.ncvc.go.jp

Our experiments have demonstrated that both carbon black (CB) and water-soluble fullerene [$C_{60}(OH)_{24}$] exhibit cytotoxicities, such as decreased cell density and cell growth, and that CB facilitates autophagic cell death in human umbilical vein endothelial cells. Furthermore, CB and $C_{60}(OH)_{24}$ up-regulate the expression of inflammation- and ubiquitin-proteasome-related genes, indicating that exposure to CB or $C_{60}(OH)_{24}$ represents a risk of atherosclerosis and ischemic heart disease (7, 8).

The results of epidemiologic and animal studies have suggested that exposure to nanoparticles plays roles in cardiovascular diseases such as atherosclerosis and myocardial infarction (2, 3, 9–12), and in genetic damage to cells or tissues (13–16). However, how exposure to airborne particulate matter induces genetic changes in germ lines or tissues is poorly understood. The small size of nanoparticles may allow them to be inhaled into the respiratory system, where they can pass into the bloodstream, ultimately reaching the germ lines. Nanomaterials then have the potential to adversely affect these cells.

Nanomaterial cytotoxicity in cells varies with chemical characteristics and surface properties, including hydrohobicity, hydrophilicity, and surface area per molecule (1, 5). Experimental studies have shown that $C_{60}(OH)_{24}$ may stimulate reactive oxygen species production in cells or tissues, and may inhibit cell proliferation or induce cell death (14). In contrast, other experimental studies have shown that $C_{60}(OH)_{24}$ may scavenge produced reactive oxygen species, and inhibit cell proliferation (17). The aim of the this study is to investigate the cytotoxic

and genotoxic effects of long-term exposure to $C_{60}(OH)_{24}$ in cultured cells. In particular, we focused on genotoxicity in germ cell [Chinese hamster ovary (CHO) cells: short G1 phase], somatic cell [human embryonic kidney 293 (HEK293) cells], and adult cell [human epidermoid-like carcinoma cells (Hela) cells: long period of G1 phase] models.

Materials and Methods

Materials

Hydroxyl fullerene {$C_{60}(OH)_{24}$; Tokyo Progress System, Tokyo, Japan} was used as described (7, 8), and its diameter was 7.1±2.4 nm.

Cell culture

All cell lines (CHO, Hela, HEK293) were obtained from Dainippon Seiyaku (Osaka, Japan) and were cultured in DMEM with 10% fetal bovine serum (Hyclone, Utah, USA). In experiments, cells were cultured in DMEM with 2% FBS and sonicated $C_{60}(OH)_{24}$ (0, 10, 100, or 1000 pg/ml or 20, 100 ng/ml). Cells were passaged every 3–4 days. Representative photomicrographs of CHO, Hela and HEK293 cells treated with $C_{60}(OH)_{24}$ had taken. CHO, Hela and HEK293 cells at ~30% confluence were treated with $C_{60}(OH)_{24}$ (0, 20, or 100 ng/ml) for 3 or 6 days.

LDH assay

Lactate dehydrogenase (LDH) activity was analyzed using a CytoTox 96 nonradioactive cytotoxicity assay kit (Promega, Madison, WI) in accordance with the manufacturer's protocols. Cells at 50–60% confluence were treated with $C_{60}(OH)_{24}$ for 33 days. LDH activity in the culture medium was evaluated on the basis of absorbance at 490 nm using a microplate reader (ARVO; PerkinElmer, Japan). Cytotoxicity was expressed relative to basal LDH release rate in untreated cells.

Proliferation assay

Cell proliferation assay was performed using a Cell Counting-8 kit (Dojindo laboratories, Kumamoto, Japan) in accordance with the manufacturer's protocols. Cells were cultured in 12-well plates and treated with $C_{60}(OH)_{24}$ (0, 10, 100, or 1000 pg/ml) for 33 days. An assay solution was added in each well, and after incubating for 3 h, the media were transferred to 96-well plates. Cell growth was measured on the basis of absorbance at 450 nm using an ARVO microplate reader.

Micronucleus test

A micronucleus test was performed in accordance with the method of Matsushima et al. (18), with slight modifications. Cells were cultured in six-well plates for 24 h, and then exposed to $C_{60}(OH)_{24}$ (0, 10, 100, or 1000 pg/ml) for 80 days. After exposure to $C_{60}(OH)_{24}$, the cells were washed 3 times with PBS, and suspended in a hypotonic solution (75 mM KCl) for 10 min at room temperature. The cells were then resuspended in cold methanol containing 25% acetic acid. After fixation, the cells were then suspended in methanol containing 1% acetic acid and spotted onto a glass slide. The cells were then air-dried and mounted with 4',6-diamido-2-phenyindole dilactate (DAPI)-containing medium. The nucleus was observed under a fluorometry microscope at 200× magnification. The number of micronucleated cells per 1000 cells was determined.

Statistical analysis

Data are presented as mean±SEM. Statistical evaluation was performed using an unpaired Student's t test. p values of <0.05 were considered to be statistically significant.

Results

We first analyzed the acute effects of exposure to relatively high doses of $C_{60}(OH)_{24}$ (0, 20, and 100 ng/ml) on cells by treating CHO, Hela and HEK293 cells with $C_{60}(OH)_{24}$ for 3 or 6 days (Fig. 1). The numbers of CHO and HEK293 cells decreased significantly in a dose-dependent manner, but the number of Hela cells did not significantly change for the 3-day exposure. The cytotoxic effects of $C_{60}(OH)_{24}$ in CHO and HEK293 cells were suppressed after 6 days; Hela cells exhibited a significantly decreased cell growth rate in a dose-dependent manner. We believe that $C_{60}(OH)_{24}$-sensitive cells died within 3 days, but $C_{60}(OH)_{24}$-resistant CHO and HEK293 cells were able to survive for 6 days. In contrast, CHO and HEK293 cells were more sensitive to ng/ml doses of $C_{60}(OH)_{24}$ than Hela cells.

To analyze the effects of very low doses of $C_{60}(OH)_{24}$ (0, 10, 100, and 1000 pg/ml), we investigated cell proliferation rate, cytotoxicity, and mitogenic effects in the three cell lines. After $C_{60}(OH)_{24}$ exposure for 33 days, the cell proliferation rates of HEK293 (peak, 1.3 fold) and Hela (peak, 2.0 fold) cells significantly increased in a dose-dependent manner (Fig. 2a). Moreover, cytotoxic effects were not observed, rather than suppressed in Hela cells under this condition (Fig. 2b). In addition, cell morphology did not change after $C_{60}(OH)_{24}$ exposure for 33 days (data not shown). These results suggest that $C_{60}(OH)_{24}$ has mitogenic rather than cytotoxic effects with long-term exposure at very low concentrations. Hela cells were more sensitive to $C_{60}(OH)_{24}$ than HEK293 cells with regard to cell growth efficiency. These results may differ owing to the cell cycle period; the G1 phase period of CHO and HEK293 cells is shorter than that of Hela cells. We hypothesized that if nanomaterials have mitogenic activity when cells are chronically exposed to $C_{60}(OH)_{24}$, abnormal nuclei such as micronuclei would be observed. After treating the cells with very low doses of $C_{60}(OH)_{24}$ for 80 days, the number of micronuclei that were stained with DAPI were determined (Fig. 3, arrowheads). The number of micronuclei was significantly higher after exposure to $C_{60}(OH)_{24}$ for 80 days than control (Fig. 4). The ratio (‰) of cells with micronuclei was also significantly high in CHO, Hela and HEK293 cells. CHO and HEK293 cells were more sensitive to $C_{60}(OH)_{24}$ than Hela cells in terms of the ratio of cells with micronuclei.

These results demonstrate that the effects of nanomaterials, such as $C_{60}(OH)_{24}$, which may have toxic, mitogenic, or mutagenetic activity, may contribute to cardiovascular diseases as well as other diseases such as cancer.

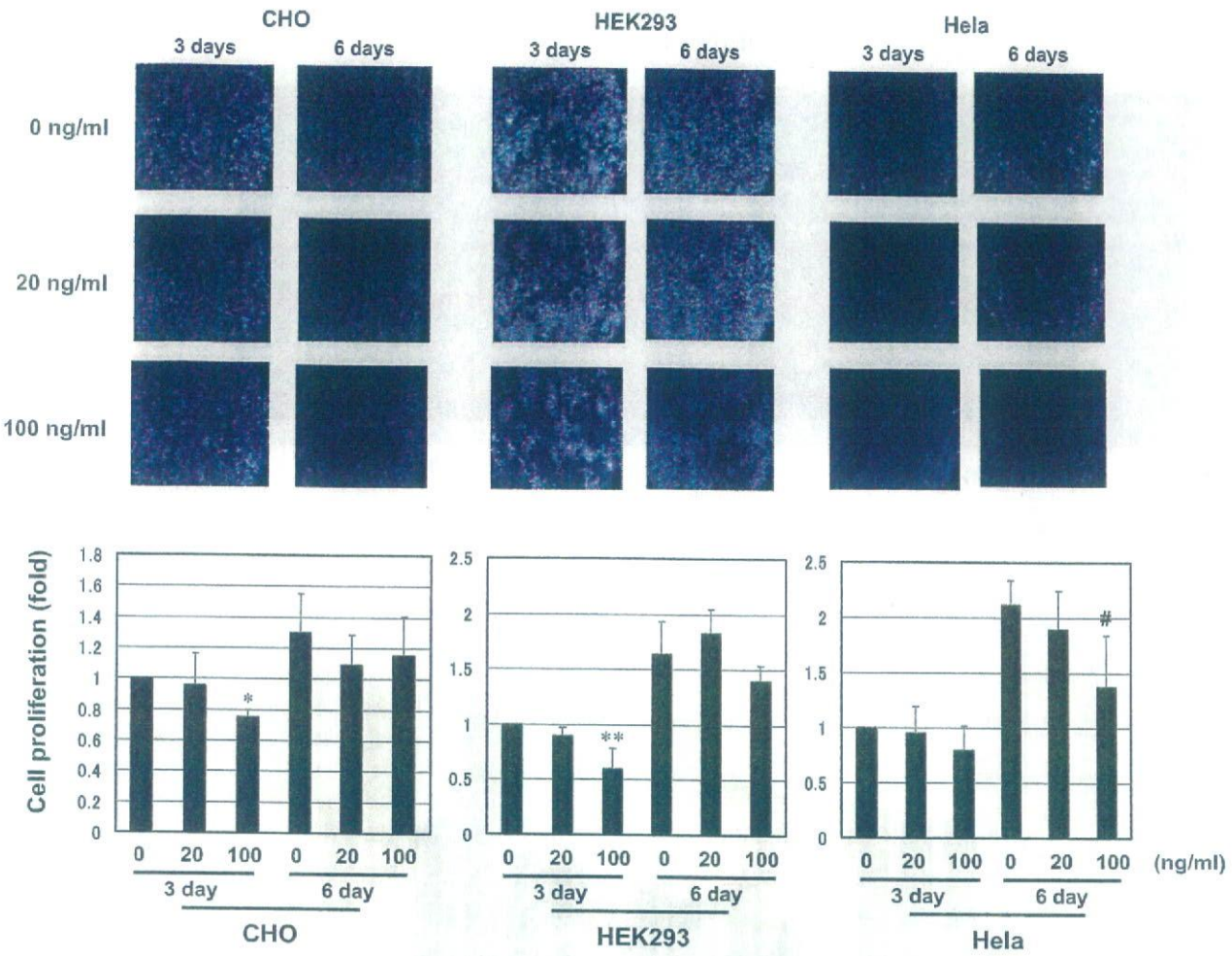

Fig. 1 Representative photomicrographs of CHO, Hela and HEK293 cells treated with $C_{60}(OH)_{24}$. CHO, Hela and HEK293 cells at ~30% confluence were treated with $C_{60}(OH)_{24}$ (0, 20, 100 ng/ml) for 3 or 6 days (upper panels). Cell number was calculated using a hemocytometer (n=4). Results are shown relative to those of controls (lower panel). * $p<0.02$, ** $p<0.03$, # $p<0.05$.

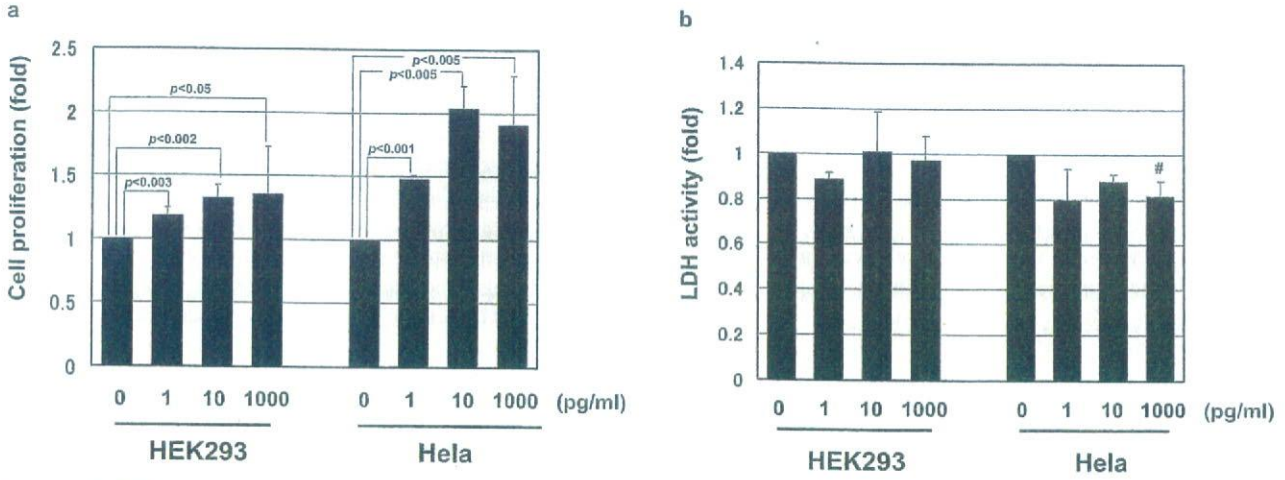

Fig. 2 $C_{60}(OH)_{24}$-induced cell growth in dose-dependent manner. HEK293 and Hela cells at ~30% confluence were treated with $C_{60}(OH)_{24}$ (0–1000 pg/ml) for 33 days. (a) The number of cells was determined using water-soluble tetrazolium salt (WST-8). (b) $C_{60}(OH)_{24}$ did not induce cytotoxic injury in HEK293 or Hela cells. Cells at ~30% confluence were treated with $C_{60}(OH)_{24}$ (0–1000 pg/ml) for 33 days. The amount of lactate dehydrogenase released into culture medium was measured. Cytotoxicity was calculated as the fold-change relative to that of the controls (n=4). Results are shown relative to those of the controls. p values indicate significance.

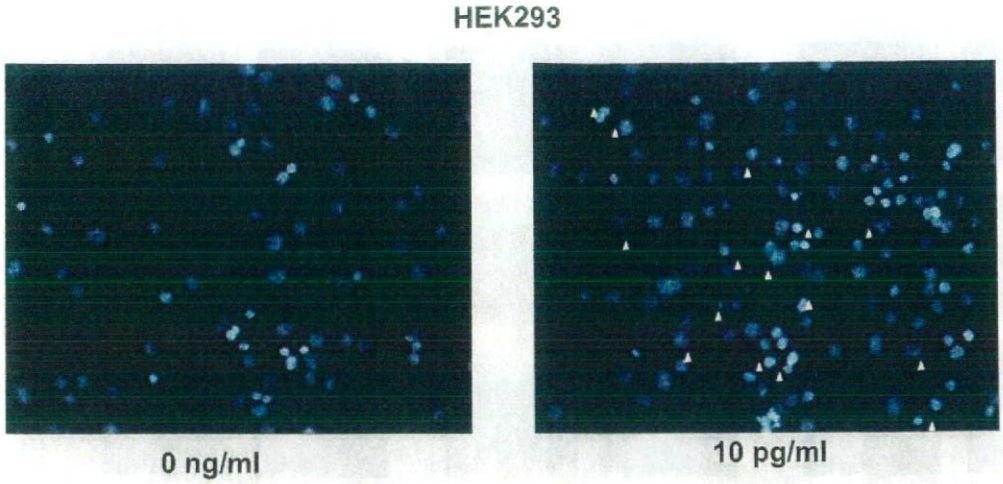

Fig. 3 The number of cells with micronuclei among HEK293 cells exposed to $C_{60}(OH)_{24}$ (0 or 10 pg/ml) for 80 days was elevated.

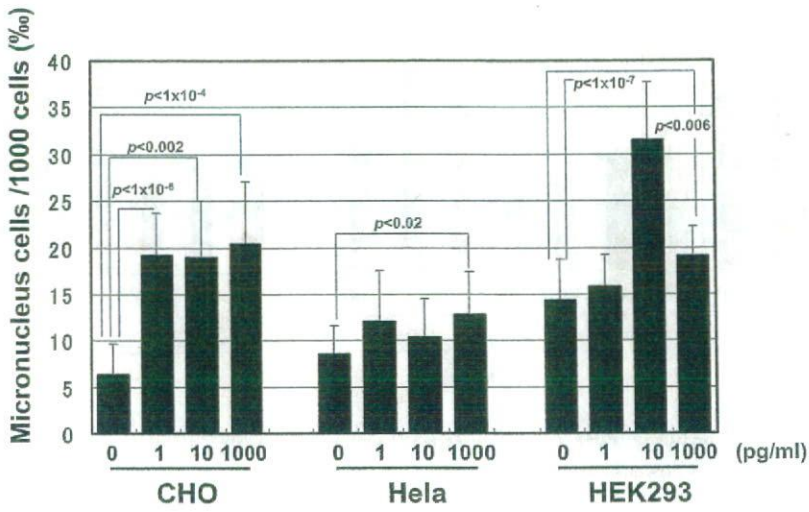

Fig. 4 Formation of micronuclei (‰) in CHO, Hela and HEK293 cells after treatment with different concentrations of $C_{60}(OH)_{24}$ for 80 days. *p* values indicate significance.

Discussion

The aim of this study is to clarify effects of chronic exposure to very low doses of nanomaterials, such as $C_{60}(OH)_{24}$, particularly with regard to genotoxicity *in vitro*. There is no evidence that pg/ml doses of $C_{60}(OH)_{24}$ have oncogenic or antioncogenic activity. Short-term exposure to relatively high doses of $C_{60}(OH)_{24}$ in the ng/ml range may induce antioncogenic functions, such as cell growth suppression (Fig. 1); however, long-term exposure to pg/ml doses of $C_{60}(OH)_{24}$ may induce cell growth (Fig. 2a). Recent studies have shown that ng/ml doses of $C_{60}(OH)_{24}$ have antioncogenic activity in various cancer cell lines (4, 19). In contrast, very low concentrations of $C_{60}(OH)_{24}$ are able to stimulate micronucleus production after long-term exposure. In this study, the cells (CHO, Hela, and HEK293) probably experienced DNA damage via an unknown mechanism (Fig. 4).

We believe that micronucleus generation caused by $C_{60}(OH)_{24}$ is not the result of chromosomal DNA damage by genotoxic molecules, such as reactive oxygen species, but is rather due to unsuccessful chromosomal DNA division during cell division during the M phase (20–22). Indeed, micronucleus production is thought to be caused when one daughter cell becomes trisomic and the other monosomic owing to aberrant segregation. The lagging chromosome may then form a micronucleus. Micronuclei can contain an entire chromosome that lags at mitosis or chromosome fragments that are not incorporated into daughter nuclei during cell division owing to kinetochore dysfunction. In addition, LDH activity was suppressed depending on the concentration of $C_{60}(OH)_{24}$ in culture medium (Fig. 2b). This shows that $C_{60}(OH)_{24}$ may scavenge reactive oxygen species, and protect against cell death. Fullerene derivatives were previously used as scavengers for reactive oxygen species, such as O_2^- and nitric oxide (17). On the basis of these results, reactive oxygen species were determined not to be involved in micronucleus generation in these experiments.

We used commercial $C_{60}(OH)_{24}$ containing about 2% (w/w) organic solvents, such as toluene. We analyzed the cytotoxic

effects of a 3-week exposure to toluene in cultured cells. At 2%, toluene did not exert any cytotoxic effects on cells (data not shown). We thus believe that $C_{60}(OH)_{24}$ stimulated a signaling pathway that influenced cell division, particularly during the period between the G2 phase and the M phase.

The results of other experiments suggest that although $C_{60}(OH)_{24}$ was used at more than 100-fold higher concentrations, both CB and $C_{60}(OH)_{24}$ induce nonapoptotic cell death mediated by the accumulation of polyubiquitinated proteins in autophagosomes, and the expression of inflammatory genes (*MCP-1*, *ICAM-1*, and *E-cadhelin*) or ubiquitin-proteasome system genes [*HECT* (a COOH-terminal catalytic homologous to E6-AP-COOH), *C2- and WW-domain-containing E3 ubiquitin protein ligase 2*, *ubiquitin-specific protease 31*, *ubiquitin-specific protease 32* and *ubiquitin-conjugating enzyme E2*] in human umbilical vein cells (7, 8). Furthermore, we demonstrated that CB and $C_{60}(OH)_{24}$ facilitate the uptake of oxidized LDL in macrophages to form foam like cells and induce the expression of the oxidized LDL receptor LOX-1 (in submission).

The kinetics of nanomaterials *in vivo* have not yet been determined. Inhaled nanoparticles are thought to be removed by alveolar macrophages via phagocytosis. By using radiolabeled water-soluble fullerene administered intravenously to rats, in which most fullerenes moved rapidly to the liver (within 1 h), it was found that fullerenes are distributed in various other tissues, including the spleen, lung, kidney, heart, and brain (23). Removal is apparently slow, with more than 90% being retained after one week, thus raising concerns about chronic toxicity. The effects of chronic exposure to nanomaterials *in vivo* thus require further examination.

Acknowledgments

This study was supported by a Health and Labor Sciences Research Grant for Research on Risk of Chemical Substance (H17-chemistry-008 to N.I.), a Grant-in-Aid for Scientific Research (#18590583 to Y.N.) from the Ministry of Education, Culture, Sports, Science, and Technology, Japan and the Program for the Promotion of Fundamental Studies in Health Science of the National Institute of Biomedical Innovation.

References

(1) Block ML, Wu X, Pei Z, Li G, Wang T, Qin L, et al. Nanometer size diesel exhaust particles are selectively toxic to dopaminergic neurons: the role of microglia, phagocytosis, and NADPH oxidase. FASEB J. 2004;18:1618–1620.

(2) Katsouyanni K, Touloumi G, Samoli E, Gryparis A, Le Tertre A, Monopolis Y, et al. Confounding and effect modification in the short-term effects of ambient particles on total mortality: results from 29 European cities within the APHEA2 project. Epidemiology. 2001;12:521–531.

(3) Nemmar A, Hoet PH, Vanquickenborne B, Dinsdale D, Thomeer M, Hoylaerts MF, et al. Passage of inhaled particles into the blood circulation in humans. Circulation. 2002;105:411–414.

(4) Tabata Y, Murakami Y, IkadaY. Photodynamic effect of polyethylene glycol-modified fullerene on tumor. Jpn J Cancer Res. 1997;88:1108–1116.

(5) Colvin VL. The potential environmental impact of engineered nanomaterials. Nat Biotechnol. 2003;21:1166–1170.

(6) Borm PJ, Kreyling W. Toxicological hazards of inhaled nanoparticles—potential implications for drug delivery. J Nanosci Nanotechnol. 2004;4:521–531.

(7) Yamawaki H, Iwai N. Mechanisms underlying nano-sized air-pollution-mediated progression of atherosclerosis: carbon black causes cytotoxic injury/inflammation and inhibits cell growth in vascular endothelial cells. Circ J. 2006;70:129–140.

(8) Yamawaki H, Iwai N. Cytotoxicity of water-soluble fullerene in vascular endothelial cells. Am J Physiol Cell Physiol. 2006;290:C1495–1502.

(9) Dockery DW, Pope CA 3rd, Xu X, Spengler JD, Ware JH, Fay ME, et al. An association between air pollution and mortality in six U.S. cities. N Engl J Med. 1993;329:1753–1759.

(10) Peters A, Dockery DW, Muller JE, Mittleman MA. Increased particulate air pollution and the triggering of myocardial infarction. Circulation. 2001;103:2810–2815.

(11) Kodavanti UP, Moyer CF, Ledbetter AD, Schladweiler MC, Costa DL, Hauser R, et al. Inhaled environmental combustion particles cause myocardial injury in the Wistar Kyoto rat. Toxicol Sci. 2003;71:237–245.

(12) Suwa T, Hogg JC, Quinlan KB, Ohgami A, Vincent R, van Eeden SF. Particulate air pollution induces progression of atherosclerosis. J Am Coll Cardiol. 2002;39:935–942.

(13) Watts RR, Lemieux PM, Grote RA, Lowans RW, Williams RW, Brooks LR, et al. Development of source testing, analytical, and mutagenicity bioassay procedures for evaluating emissions from municipal and hospital waste combustors. Environ Health Perspect. 1992;98:227–234.

(14) Rancan F, Rosan S, Boehm K, Fernandez E, Hidalgo ME, et al. Cytotoxicity and photocytotoxicity of a dendritic C(60) mono-adduct and a malonic acid C(60) tris-adduct on Jurkat cells. J Photochem Photobiol B. 2002;67:157–162.

(15) Soares SR, Bueno-Guimaraes HM, Ferreira CM, Rivero DH, De Castro I, Garcia ML, et al. Urban air pollution induces micronuclei in peripheral erythrocytes of mice in vivo. Environ Res. 2003;92:191–196.

(16) Somers CM, McCarry BE, Malek F, Quinn JS. Reduction of particulate air pollution lowers the risk of heritable mutations in mice. Science. 2004;304:1008–1010.

(17) Mirkov SM, Djordjevic AN, Andric NL, Andric SA, Kostic TS, Bogdanovic GM, et al. Nitric oxide-scavenging activity of polyhydroxylated fullerenol, C60(OH)24. Nitric Oxide. 2004;11:201–207.

(18) Matsushima T, Hayashi M, Matsuoka A, Ishidate M Jr, Miura KF, Shimizu Y, et al. Validation study of the in vitro micronucleus test in a Chinese hamster lung cell line (CHL/IU). Mutagenesis. 1999;14:569–580.

(19) Kamat JP, Devasagayam TP, Priyadarsini KI, Mohan H. Reactive oxygen species mediated membrane damage induced by fullerene derivatives and its possible biological implications. Toxicology. 2000;155:55–61.

(20) Antoccia A, Tanzarella C, Modesti D, Degrassi F. Cytokinesis-

block micronucleus assay with kinetochore detection in colchicine-treated human fibroblasts. Mutat Res. 1993;287: 93–99.

(21) Cimini D, Tanzarella C, Degrassi F. Differences in malsegregation rates obtained by scoring ana-telophases or binucleate cells. Mutagenesis. 1999;14:563–568.

(22) Kirsch-Volders M, Elhajouji A, Cundari E, Van Hummelen P. The in vitro micronucleus test: a multi-endpoint assay to detect simultaneously mitotic delay, apoptosis, chromosome breakage, chromosome loss and non-disjunction. Mutat Res. 1997;392:19–30.

(23) Yamago S, Tokuyama H, Nakamura E, Kikuchi K, Kananishi S, Sueki K, et al. In vivo biological behavior of a water-miscible fullerene: 14C labeling, absorption, distribution, excretion and acute toxicity. Chem Biol. 1995;2:385–389.

Circ J 2007; **71:** 191–195

Characterization of Subclinical Thyroid Dysfunction From Cardiovascular and Metabolic Viewpoints

— The Suita Study —

Naoyuki Takashima, MD; Yasuharu Niwa, PhD; Toshifumi Mannami, MD*,**; Hitonobu Tomoike, MD*; Naoharu Iwai, MD

Background Subclinical hypothyroidism, defined as high serum thyroid-stimulating hormone (TSH) levels and normal serum free-triiodothyronine (fT3) and serum free-thyroxine (fT4) levels, is a common medical problem among the elderly, but it is unclear whether it should be treated with thyroid hormone replacement therapy.
Methods and Results A cross-sectional study of 3,607 participants in a community health survey in Suita, in the northern part of Osaka, was performed. Participants were categorized into 5 groups: normal, hyperthyroidism, hypothyroidism, subclinical hypothyroidism, and subclinical hyperthyroidism. The association between each group and various phenotypes was examined, in relation to cardiovascular disease and metabolic syndromes. Serum TSH levels increased and fT3 and fT4 levels decreased with age. A total of 14.6% of subjects aged 70–80 years and 20.1% of subjects aged older than 80 years were classified as having subclinical hypothyroidism. Subclinical hypothyroidism was not associated with glycol-hemoglobin A1c, body mass index, pulse rate, hypertension, total cholesterol, high-density lipoprotein cholesterol or triglyceride levels or intima–media thickness. It was only associated with higher fasting blood glucose and glycol-hemoglobin A1c levels compared with euthyroidism.
Conclusions The present observation does not support the need for treatment of subclinical hypothyroidism or subclinical hyperthyroidism. (*Circ J* 2007; **71:** 191–195)

Key Words: Blood sugar; Diabetes; Lipids; Subclinical hyperthyroidism; Subclinical hypothyroidism

Subclinical hypothyroidism (SCH), defined as high serum thyroid-stimulating hormone (TSH) levels and normal levels of serum free-triiodothyronine (fT3) and serum free-thyroxine (fT4), is a common medical problem among the elderly. The prevalence of SCH has been reported to be 4–10% in the general population and up to 20% in women older than 60 years[1–3] The incidence of SCH is 2.1–3.8% per year in thyroid-antibody-positive subjects and 0.3% per year in thyroid-antibody-negative subjects[4]

Serum lipid levels in SCH have been reported as either normal[5] or elevated[6,7] In the Tromsø study, low-density lipoprotein-cholesterol (LDL-C) levels were significantly higher in subjects with SCH compared with controls[7] and, moreover, they were reduced with thyroxine treatment. In addition, associations between left ventricular function and SCH have been widely investigated, but the findings are controversial. Some studies have shown an association between SCH and poor left ventricular function and others have not[8] Moreover, the positive association between arterial stiffness and hypothyroidism, even in the subclinical stage, has been reported[9,10] Subclinical hyperthyroidism has been associated with a higher prevalence of atrial fibrillation (AF) and increased heart rate[8] but not with elevated serum lipid levels[6]

(Received August 17, 2006; revised manuscript received October 31, 2006; accepted November 20, 2006)
*Departments of Epidemiology, *Preventive Cardiology, National Cardiovascular Center, Suita and **Hygiene and Public Health, Social Medicine, Faculty of Medicine, Kagawa University, Kagawa, Japan*
Mailing address: Naoyuki Takashima, MD, Department of Epidemiology, National Cardiovascular Center, 5-7-1 Fujishirodai, Suita 565-8565, Japan. E-mail: ntaka@ri.ncvc.go.jp

In the present study we investigated whether subclinical thyroid dysfunction in Japanese individuals is associated with various phenotypes related to cardiovascular disease and metabolic syndromes.

Methods

Study Population

The selection criteria and design of the Suita study have been described previously[11–13] Serum TSH, fT3, and fT4 levels were measured in 3,607 subjects who were not being treated for thyroid disease. The present study was approved by the Ethics Committee of the National Cardiovascular Center, and all subjects provided written informed consent. We categorized patients into 5 groups: normal (normal levels of serum TSH [0.436–3.78 μU/ml], fT3 [2.1–4.1 pg/ml] and fT4 [1.0–1.7 ng/dl]), hyperthyroidism (low levels of TSH and high levels of fT3 and/or fT4), hypothyroidism (high levels of TSH and low levels of fT3 and/or fT4), SCH (high levels of TSH and normal levels of fT3 and fT4), and subclinical hyperthyroidism (low levels of TSH and normal levels of fT3 and fT4)[14] Body mass index (BMI) was calculated as body weight (kg) divided by height in square meters.

The intima–media thickness (IMT) was measured on longitudinal scan of the common carotid artery at a point 10 mm proximal from the beginning of the dilation of the bulb[11]

Serum TSH, fT3, and fT4 Levels

Fasting serum samples were collected at study entry and stored at –80°C until tests were run. Serum TSH was mea-

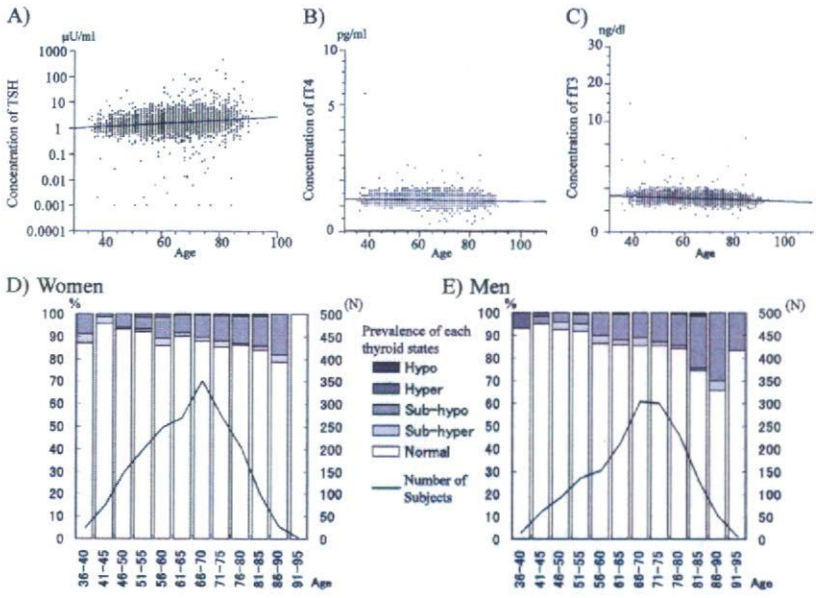

Fig 1. Serum TSH, fT3, and fT4 hormone levels and age. (A–C) Correlation between serum TSH (A), fT3 (B), and fT4 levels (C) and age are plotted (grey dot). Serum TSH levels increased with age. There was a linear correlation between log transferred serum TSH levels and age. Serum fT3 and fT4 levels decreased with age. There was a linear correlation between these thyroid hormone levels and age ($p<0.01$). (D–E) The prevalence of women (D) and men (E) in each thyroid state according to age is shown. The total number of subjects according to age is shown by the black line. The prevalence of subclinical hypothyroid in both men and women increased with age. However the prevalence of subclinical hyperthyroidism did not increase with age. TSH thyroid-stimulating hormone; fT3, serum free-triiodothyronine; fT4 serum free-thyroxine.

sured by a chemiluminescent immunoassay kit (Mitsubishi Kagaku BCL, Abbott Laboratories, Chicago, IL, USA), as were serum fT3 and fT4 levels (Mitsubishi Kagaku BCL, Bayer, Leverkusen, Germany).

Statistical Analysis

Values are expressed as mean±standard deviation. All statistical analyses were performed with the JMP statistical package (SAS Institute Inc, Cary, NC, USA). One-way analysis of variance tests were used to determine whether an association existed among thyroid status and BMI (adjusted for age and sex), systolic and diastolic blood pressures (SBP: adjusted for age, BMI, and sex; DBP: adjusted for age, BMI, and sex), pulse rate (PR; adjusted for age and sex), glycol-hemoglobin A1c (HbA1c: adjusted for age, BMI, and sex), fasting blood glucose levels (FBG: adjusted for age, BMI, and sex), high-density lipoprotein (HDL: adjusted for cholesterol BMI, sex, age, number of cigarettes/day, and alcohol consumption [g/day]), total cholesterol (TC: adjusted for age, BMI, and sex), triglycerides (TG: adjusted for age, BMI, and sex) and IMT. Simple correlation analyses were used to determine whether an association existed between normal states and each thyroid state, as well as between the variables assessed after adjusting for confounding factors. Logistic analysis was used to determine whether an association existed among thyroid status and the prevalence of AF.

Results

Serum concentrations of TSH increased and serum concentrations of fT3 and fT4 decreased with age (Figs 1A–C). Similarly, the number of men and women with SCH also increased with age (Figs 1D,E). Overall, 11.6% of women aged 71–80 years and 13.8% of women aged older than 80 years were classified into the SCH category (Fig 1D). For men, 13.4% aged 71–80 years and 24.5% older than 80 years were classified into the SCH category (Fig 1E).

The characteristics of the study population are shown in Table 1. Participants included 3,130 normal subjects, 19 with hyperthyroidism, 4 with hypothyroidism, 77 with subclinical hyperthyroidism, and 377 with SCH. The prevalence of SCH was 10.45% and that of subclinical hyperthyroidism was 2.13%. Compared with normal individuals, subjects with SCH were significantly older (69.02±10.43 years vs 64.22±11.29 years, respectively; $p<0.05$) and had significantly lower serum fT3 levels (2.99±0.33 ng/dl vs 3.12±0.32 ng/dl, respectively; $p<0.01$, adjusted for age and sex) and fT4 levels (1.09±0.19 pg/ml vs 1.24±0.15 pg/ml, respectively; $p<0.01$, adjusted for age and sex). On the other hand, when individuals with subclinical hyperthyroidism were compared with normal subjects, they showed significantly higher concentrations of fT4 (1.34±0.18 pg/ml vs 1.24±0.15 pg/ml, respectively; $p<0.01$, adjusted for age and sex). Subjects with overt hyperthyroidism had significantly lower HDL ($p<0.01$) and TC levels ($p<0.01$) and higher PR ($p<0.01$) than subjects with normal thyroid function. Subjects with overt hypothyroidism had significantly higher TC levels ($p<0.01$) than subjects with normal thyroid function. Characteristics associated with hyper- and hypothyroid subjects were as reported previously[15]

Characteristics of subjects with normal and subclinical thyroid dysfunction are shown in Table 2. The PR among subjects not being treated for arrhythmia was not significantly associated with subclinical hyperthyroidism or SCH after adjusting for age and sex. Blood pressure among subjects not being treated for hypertension was not significantly associated with subclinical hyperthyroidism or SCH after adjusting for appropriate confounding factors. Among subjects not being treated for hypertriglyceridemia, TG levels were not significantly associated with subclinical hyperthyroidism or SCH compared with normal subjects. HDL-cholesterol and TC levels were not significantly associated with subclinical hyperthyroidism or SCH subjects not being treated for hyperlipidemia. Among all subjects not receiving treatment for diabetes, FBG was significantly associated with SCH ($p<0.01$). Subjects with subclinical hyperthyroidism had significantly higher HbA1c ($p<0.05$) and FBG ($p<0.01$) levels than normal subjects. The numbers of subjects not being treated for each disease is shown in Table 2.

The prevalence of AF in subjects with subclinical hyper-

Table 1 Characteristics of the Study Population

	Normal thyroid	Hyperthyroidism	Hypothyroidism	Subclinical hyperthyroidism	Subclinical hypothyroidism	Total
N (%)	3,130 (86.78)	19 (0.53)	4 (0.11)	77 (2.13)	377 (10.45)	3,607 (100)
Male (%)	1,442 (46.07)	5 (26.32)	3 (75.0)	39 (50.65)	203 (53.85)	1,692 (44.55)
Age (years)	64.22±11.29	62.16±12.85	76.50±8.43	63.94±10.85	69.02±10.43‡	64.70±11.29
BMI	22.82±3.11	22.73±3.48	24.02±0.58	22.77±3.03	22.84±3.34	22.82±3.14
SBP (mmHg)	129.24±19.65	131.32±20.63	135.50±10.47	125.57±15.45	131.93±19.06	129.41±19.69
DBP (mmHg)	77.82±10.09	76.11±11.95	71.50±15.37	75.03±10.76	77.97±9.61	77.74±10.17
PR (beats/min)§	66.10±8.25	72.42±9.74‡	62.00±3.27	67.12±9.38	66.51±8.35	66.20±8.38
FBG (mg/dl)¶	99.75±21.32	105.16±40.89	99.00±4.97	106.79±38.83†	98.64±18.68	99.79±21.67
HbA1c (%)¶	5.49±0.74	5.47±0.86	5.57±0.31	5.73±1.49†	5.54±0.77	5.50±0.77
HDL-C (mg/dl)	60.56±15.52	51.11±15.81‡	55.25±16.80	58.71±17.01	58.47±16.01	60.20±15.61
TC (mg/dl)	208.26±32.09	185.58±35.83‡	247.25±55.05†	206.79±33.26	206.34±35.48	207.99±32.53
TG (mg/dl)	106.90±74.77	111.74±64.30	156.00±61.36	123.12±72.03	113.30±69.72	108.16±74.59
Prevalence of MI (%)	40 (1.28)	0 (0.00)	0 (0.00)	2 (2.60)	7 (1.86)	49 (1.36)
Prevalence of CVA (%)	89 (2.84)	0 (0.00)	0 (0.00)	3 (3.90)	13 (3.45)	105 (2.91)
Prevalence of AF (%)	44 (1.41)	0 (0.00)	0 (0.00)	2 (2.60)	15 (3.98)	61 (1.69)
TSH (μU/ml)	1.723±0.824	0.10±0.20	209.85±171.57‡	0.27±0.13*	8.32±11.42‡	2.60±9.51
fT4 (ng/dl)	1.24±0.15	2.26±0.97‡	0.35±0.0‡	1.34±0.18†	1.09±0.19‡	1.23±0.20
fT3 (pg/ml)	3.12±0.32	6.75±5.77‡	1.65±0.29‡	3.18±0.46	2.99±0.33‡	3.12±0.59

†$p<0.05$ and ‡$p<0.01$.
P values are for comparisons with normal thyroid subjects after adjustment for appropriate confounding factors.
Values are mean±standard deviation.
§Number of patients treated for arrhythmia was 61 in normal subjects, 1 in subclinical hyperthyroidism subjects, and 9 in subclinical hypothyroidism subjects; ¶number of patients treated for diabetes was 150 in normal subjects, 1 in hyperthyroidism subjects, 7 in subclinical hyperthyroidism subjects, and 22 in subclinical hypothyroidism subjects.
BMI, body mass index; SBP, systolic blood pressure; DBP, diastolic blood pressure; PR, pulse rate; FBG, fasting blood glucose levels; Hb, hemoglobin; HDL, high-density lipoprotein; C, cholesterol; TC, total cholesterol; TG, triglyceride; MI, myocardial infraction; CVA, cerebrovascular accident; AF, atrial fibrillation; TSH, thyroid-stimulating hormone; fT4, free-thyroxine; fT3, free-triiodothyronine.

Table 2 Characteristics of the Subjects in the Normal and Subclinical Thyroidism Groups

	Normal thyroid	Subclinical hyperthyroidism	Subclinical hypothyroidism	ANOVA p-value**
N	3,130	77	377	
BMI	22.82±3.11	22.77±3.03	22.84±3.34	NS
N‡	2,355	57	270	
SBP (mmHg)	124.95±18.37	122.53±20.00	127.74±17.98	NS
DBP (mmHg)	76.67±9.98	73.49±10.99	76.93±9.50	NS
N§	3,057	75	364	
PR (beats/min)	66.12±8.23	67.33±9.40	66.47±8.27	NS
N¶	2,976	70	355	
HbA1c	5.40±0.56	5.56±1.34*	5.41±0.48	<0.05
FBG (mg/dl)	97.07±15.27	103.6±36.73†	95.58±11.57†	<0.0001
N††	3,084	73	371	
TG (mg/dl)	105.95±74.12	121.52±75.98	112.73±69.70	NS
N‖	2,726	63	320	
HDL (mg/dl)	60.58±15.65	58.40±17.36	58.37±16.41	NS
TC (mg/dl)	207.78±32.47	207.40±34.81	205.44±36.39	NS

*<0.05 and †<0.01.
**P values are for comparisons with normal thyroid subjects after adjustment for appropriate confounding factors.*
Values are mean±standard deviation.
‡Without treatment for hypertension; §without treatment for arrhythmia; ¶without treatment for diabetes mellitus; ††without treatment for hypertriglyceridemia; ‖without treatment for hyperlipidemia.
ANOVA, analysis of variance. Other abbreviations see in Table 1.

thyroidism was higher than that in normal subjects (3.98% vs 1.41%) but the difference was not statistically significant. Subjects who had been diagnosed with AF were included with those with AF.

A total of 12% of subjects with SCH had high serum TSH levels (>10μU/ml). Subjects with SCH and TSH levels >10μU/ml were older than subjects with SCH and TSH levels =10μU/ml (67.28±9.62 years vs 71.07±9.70 years, $p<0.05$). Subjects with SCH and high TSH levels (>10μU/ml) did not have lower FBG, HbA1c or lipid levels compared with normal subjects (unpubl. data).

The correlation between laboratory data and fT3, fT4, and TSH levels in normal subjects is shown in Table 3. Serum fT4 and fT3 levels in normal subjects were significantly associated with various laboratory data after adjusting for appropriate confounding factors.

We examined whether an association between IMT and thyroid dysfunction existed (Table 4). There were weak associations between thyroid states and IMT-mean, and IMT-max, but these disappeared after adjusting for age and sex. Multiple logistic analysis did not detect a significant correlation between thyroid state (normal or subclinical

Table 3 Correlation Between Laboratory Data and Thyroid Hormone Level in Normal Subjects

Thyroid state	*TG*[††]	*FBG*[¶]	*HbA1c*[¶]	*TC*[‖]	*HDL*[‖]	*BMI*	*PR*[§]	*SBP*[‡]	*DBP*[‡]
No. of subjects	*3,084*	*2,976*	*2,976*	*2,726*	*2,726*	*3,130*	*3,057*	*2,355*	*2,355*
TSH									
P	*0.0015*	*NS*	*NS*	*0.015*	*0.0055*	*NS*	*NS*	*NS*	*NS*
*	*5.21*	*0.20*	*0.0090*	*1.83*	*–0.92*	*0.045*	*–0.10*	*–0.24*	*0.12*
Normal thyroid									
fT3									
P	*0.0043*	*NS*	*NS*	*NS*	*<0.0001*	*<0.0001*	*NS*	*NS*	*NS*
*	*12.16*	*0.15*	*–0.023*	*0.22*	*–4.01*	*1.06*	*0.12*	*1.75*	*0.64*
fT4									
P	*0.039*	*0.0006*	*0.030*	*0.0010*	*0.071*	*NS*	*<0.0001*	*0.002*	*0.023*
*	*18.00*	*6.03*	*0.14*	*13.09*	*3.16*	*0.43*	*4.83*	*7.06*	*2.95*

**Correlation coefficient with each value.*
P values are coefficient of correlation; p values are for comparisons with normal thyroid subjects after adjustment for appropriate confounding factors.
[‡]Without treatment for hypertension; [§]without treatment for arrhythmia; [¶]without treatment for diabetes mellitus; [‖]without treatment for hypertriglyceridemia; [‖]without treatment for hyperlipidemia.
Abbreviations see in Table 1.

Table 4 Correlation Between Thyroid Status and IMT

	Normal thyroid	*Hyperthyroidism*	*Hypothyroidism*	*Subclinical hyperthyroidism*	*Subclinical hypothyroidism*	*ANOVA p value*
N	*2,819*	*17*	*4*	*65*	*321*	
IMT-max (mm)	*1.30±0.55*	*1.21±0.63*	*1.73±0.97*	*1.25±0.53*	*1.40±0.58*	*0.048*
*Residual IMT-max**	*0.002±0.491*	*–0.015±0.492*	*0.089±0.892*	*–0.052±0.467*	*–0.009±0.520*	*0.892*
Residual IMT-max[†]	*0.001±0.784*	*–0.046±0.506*	*0.094±0.855*	*–0.064±0.463*	*–0.001±0.510*	*0.786*
N	*2,818*	*17*	*4*	*65*	*320*	
IMT-mean (mm)	*0.821±0.13*	*0.79±0.13*	*0.93±0.09*	*0.83±0.13*	*0.83±0.13*	*0.042*
*Residual IMT-mean**	*0.0004±0.105*	*–0.004±0.108*	*0.022±0.496*	*0.018±0.118*	*–0.008±0.112*	*0.581*
Residual IMT-mean[†]	*0.000±0.103*	*–0.301±0.103*	*0.014±0.035*	*0.014±0.111*	*–0.005±0.110*	*0.821*

Values are mean±standard deviation.
**Aadjusted for age and sex; [†]adjusted by age, BMI, SBP, FBS, number of cigarettes/day, TG, TC and HDL.*
IMT, intima–media thickness. Other abbreviations see in Tables 1,2.

thyroid dysfunction) and the prevalence of atherosclerotic vascular diseases, such as cerebral infarction, transient cerebral ischemic attack, cerebral stroke, acute myocardial infarction and angina pectoris (p=0.090, unpubl. data).

Discussion

In this large cross-sectional study of subclinical thyroid dysfunction in Japanese subjects, although the prevalence of SCH increased with age overall, the prevalence of SCH in elderly patients was lower than that reported in other studies, particularly in women: 18.8% for men older than 75 years and 12.7% for women older than 75 years. This finding differs from that of previous studies in which the prevalence of SCH was higher in elderly women than in elderly men[1,3,6] In the Colorado study, the prevalence of SCH was 16% in men older than 75 years and 21% in women older than 75 years! The differences in these trends might be due to different genetic, ethnic or environmental backgrounds of the subjects. On the other hand, the prevalence of subclinical hyperthyroidism was 2.13% in our study, which is similar to that in the Colorado study (2.1%)!

We found that the presence of SCH was associated with lower FBG levels and that subclinical hyperthyroidism was associated with higher FBG and HbA1c levels. Moreover, our results also indicate that thyroid hormone levels in normal subjects are significantly associated with various laboratory data, including FBG and HbA1c levels. Compared with normal subjects, serum thyroid hormone levels in subjects with SCH were lower and levels in subjects with subclinical hyperthyroidism were higher. Therefore, lower or higher levels of thyroid hormone (within the normal range) in subclinical thyroid dysfunction might influence glucose metabolism.

We did not observe any significant association between subclinical thyroid dysfunction and lipid metabolism, which was consistent with a previous US study[5] However, other studies in Norway and Australia have reported dyslipidemia in subjects with SCH[6,7] We examined whether higher TSH levels (>10μU/ml) in subjects with SCH were associated with lipid metabolism, but did not find any significant association between lipid metabolism and TSH levels >10μU/ml in subjects with SCH compared with normal subjects. Moreover, higher TSH levels did not show any association with FBG levels. These results might be related to aging, because hypofunction of the endocrine glands occurs with age. Serum lipid, FBG, and HbA1c levels were sustained in subjects with high TSH levels and SCH.

We did not observe any significant association between subclinical thyroid dysfunction and IMT, which suggests that subclinical thyroid dysfunction might not be related to an increased risk of atherosclerosis. Moreover, we did not find any significant association between SCH and previous history of arteriosclerotic vascular diseases. However, this result was not consistent with previous studies[8,10] possibly because of the size of our study population and different

surrogate markers for atherosclerosis.

The necessity for thyroid hormone replacements therapy for SCH is not supported by the present study results. The signs and symptoms of hypothyroidism are bradycardia, mild hypertension and hyperlipidemia, which might accelerate atherosclerosis in subjects with hypothyroidism.[1,6] We examined the association between SCH and these symptoms or signs and did not observe an association between SCH and blood pressure or serum lipid levels. The association between lipid profile and SCH has been previously reported in Norway and Australia[6,7] and the different results might relate to differences in genetic background, life style and BMI. In the Tromsø study,[7] the subjects were obese and those with SCH were even more obese than normal subjects. The difference in BMI between those and our investigations might induce different patterns of lipid metabolism. We did not observe any significant association between SCH and the symptoms or signs associated with hypothyroidism. Moreover, we did not find an association between SCH and IMT, as a surrogate marker for atherosclerosis, and did not find an association between SCN and past history of atherosclerotic disease. These results do not support the need for treatment of SCH in Japanese subjects. However, our investigation was a cross-sectional study, so the duration of SCH was not considered in the analysis. Our results do not completely deny that subjects with long-term SCH have increased risk of atherosclerosis.

In conclusion, we examined the association between subclinical thyroid dysfunction and various factors in a general population. We only found an association between glucose levels and subclinical thyroid dysfunction. The differences in serum glucose levels among the thyroid states (SCH, subclinical hyperthyroidism, and normal thyroid) were too small to lead to a recommendation for treatment of subclinical thyroid dysfunction and thus do not indicate a need for treatment of subclinical thyroid dysfunction in Japanese subjects.

Acknowledgements

This study was supported by a grant from the Program for Promotion of Fundamental Studies in Health Science of the National Institute of Biomedical Innovation. We acknowledge the contribution of the members of this study.

References

1. Canaris GJ, Manowitz NR, Mayor G, Ridgway EC. The Colorado thyroid disease prevalence study. *Arch Intern Med* 2000; **160:** 526–534.
2. Gharib H, Tuttle RM, Baskin HJ, Fish LH, Singer PA, McDermott MT. Subclinical thyroid dysfunction: A joint statement on management from the American Association of Clinical Endocrinologists, the American Thyroid Association, and the Endocrine Society. *J Clin Endocrinol Metab* 2005; **90:** 581–585; discussion 586–587.
3. Sawin CT, Castelli WP, Hershman JM, McNamara P, Bacharach P. The aging thyroid: Thyroid deficiency in the Framingham Study. *Arch Intern Med* 1985; **145:** 1386–1388.
4. Samuels MH. Subclinical thyroid disease in the elderly. *Thyroid* 1998; **8:** 803–813.
5. Hueston WJ, Pearson WS. Subclinical hypothyroidism and the risk of hypercholesterolemia. *Ann Fam Med* 2004; **2:** 351–355.
6. Walsh JP, Bremner AP, Bulsara MK, O'Leary P, Leedman PJ, Feddema P, et al. Thyroid dysfunction and serum lipids: A community-based study. *Clin Endocrinol (Oxf)* 2005; **63:** 670–675.
7. Iqbal A, Jorde R, Figenschau Y. Serum lipid levels in relation to serum thyroid stimulating hormone and the effect of thyroxine treatment on serum lipid levels 7 in subjects with subclinical hypothyroidism: The Tromso Study. *J Intern Med* 2006; **260:** 53–61.
8. Biondi B, Palmieri EA, Lombardi G, Fazio S. Effects of subclinical thyroid dysfunction on the heart. *Ann Intern Med* 2002; **137:** 904–914.
9. Dagre AG, Lekakis JP, Papaioannou TG, Papamichael CM, Koutras DA, Stamatelopoulos SF, et al. Arterial stiffness is increased in subjects with hypothyroidism. *Int J Cardiol* 2005; **103:** 1–6.
10. Biondi B, Klein I. Hypothyroidism as a risk factor for cardiovascular disease. *Endocrine* 2004; **24:** 1–13.
11. Mannami T, Konishi M, Baba S, Nishi N, Terao A. Prevalence of asymptomatic carotid atherosclerotic lesions detected by high-resolution ultrasonography and its relation to cardiovascular risk factors in the general population of a Japanese city: The Suita study. *Stroke* 1997; **28:** 518–525.
12. Iwai N, Katsuya T, Mannami T, Higaki J, Ogihara T, Kokame K, et al. Association between SAH, an acyl-CoA synthetase gene, and hypertriglyceridemia, obesity, and hypertension. *Circulation* 2002; **105:** 41–47.
13. Kokubo Y, Iwai N, Tago N, Inamoto N, Okayama A, Yamawaki H, et al. Association analysis between hypertension and CYBA, CLCNKB, and KCNMB1 functional polymorphisms in the Japanese population: The Suita Study. *Circ J* 2005; **69:** 138–142.
14. Surks MI, Ortiz E, Daniels GH, Sawin CT, Col NF, Cobin RH, et al. Subclinical thyroid disease: Scientific review and guidelines for diagnosis and management. *JAMA* 2004; **291:** 228–238.
15. Dillmann WH. The thyroid. *In*: Bennett JC, editor. Cecil textbook of medicine, 20th edn. Philadelphia: WB Saunders; 1996; 1227–1245.
16. Irwin K, Kaie O. Thyroid hormone and the cardiovascular system. *N Engl J Med* 2001; **344:** 501–509.

Circ J 2007; **71:** 437–444

Nanomaterials Induce Oxidized Low-Density Lipoprotein Cellular Uptake in Macrophages and Platelet Aggregation

Yasuharu Niwa, PhD; Naoharu Iwai, MD

Background Nanomaterials have numerous potential benefits for society, but the potential hazards of nanomaterials on human health are poorly understood. Nanomaterials are known to pass into the circulatory system in humans, causing vascular injuries that might play a role in the development of atherosclerosis. The present study aimed to determine the effects of chronic exposure to nanomaterials on macrophage phenotype and platelet aggregation.

Methods and Results Cultured macrophages (RAW264.7) were treated with carbon black (CB) and water-soluble fullerene ($C_{60}(OH)_{24}$) from 7 to 50 days. Individually, CB had no significant effects on RAW264.7 cell growth, whereas $C_{60}(OH)_{24}$ alone or CB and $C_{60}(OH)_{24}$ together with oxidized low-density lipoprotein (Ox-LDL) (100 μg/ml) induced cytotoxic morphological changes, such as Ox-LDL uptake-induced foam cell-like formation and decreased cell growth, in a dose-dependent manner. $C_{60}(OH)_{24}$ induced LOX-1 protein expression, pro-matrix metalloprotease-9 protein secretion, and tissue factor mRNA expression in lipid-laden macrophages. Although CB or $C_{60}(OH)_{24}$ alone did not induce platelet aggregation, $C_{60}(OH)_{24}$ facilitated adenosine diphosphate (ADP)-induced platelet aggregation. Furthermore, $C_{60}(OH)_{24}$ acted as a competitive inhibitor of ADP receptor antagonists in ADP-mediated platelet aggregation.

Conclusions The present study confirmed novel effects of nanomaterials in macrophages and platelets. These effects suggest that exposure to nanomaterials might be a risk for atherothrombotic diseases. (*Circ J* 2007; **71:** 437–444)

Key Words: Atherosclerosis; Lipid-laden macrophages; Nanomaterials; Platelet aggregation

The advent of nanomaterials has provided incredible opportunities for biomedical applications such as therapeutic and diagnostic tools, in addition to applications in engineering, electronics and optics[1–3] Biomedical applications under development include targeted drug delivery systems for the brain and tumor tissues and intravascular nanosensor and nanorobotic devices for imaging and diagnosis. However, the potential adverse effects of nanomaterials on human health remains to be established[4–6]

Potential exposure pathways for nanomaterials have been proposed in humans[5,7] Although inhalation might be a major route of exposure, ingestion and dermal exposure are also possible during the nanomaterial manufacture. After inhalation, nanomaterials are deposited in the respiratory tract, and their small size allows cellular uptake and transcytosis into the blood and lymphatic system. Our experiments have shown that both carbon black (CB) and water-soluble fullerene ($C_{60}(OH)_{24}$) exhibit cytotoxicity in human umbilical vein endothelial cells (HUVEC), such as decreased cell density and cell growth. Furthermore, CB and $C_{60}(OH)_{24}$ upregulated the expression of inflammation-related genes and ubiquitin-proteasome-related genes in HUVEC. These results suggest that exposure to CB and/or $C_{60}(OH)_{24}$ might be a risk for atherothrombotic diseases[8,9]

(Received June 13, 2006; revised manuscript received December 6, 2006; accepted December 19, 2006)

Department of Epidemiology, Research Institute, National Cardiovascular Center, Suita, Japan

Mailing address: Yasuharu Niwa, PhD, Department of Epidemiology, Research Institute, National Cardiovascular Center, Suita 565-8565, Japan. E-mail: yniwa@ri.ncvc.go.jp

In addition to endothelium, macrophages and platelets are important players for atherogenesis. Macrophages under the endothelium may take up denatured-low-density lipoprotein (LDL) (oxidized-LDL; Ox-LDL and acetylated-LDL; Ac-LDL) and become foam cells. The lipid-laden macrophages play a key role in inducing plaque rupture by secreting proteases, such as a matrix metalloprotease-9 (MMP-9) that destroys the extracellular matrix. Finally, rupture of advanced atherosclerotic plaques can lead to platelet aggregation, which results in atherothrombotic events.

In the present study, we aimed to clarify the effects of chronic exposure of nanomaterials, such as CB and $C_{60}(OH)_{24}$, on macrophages phenotypes and the aggregating effects of CB and $C_{60}(OH)_{24}$ on platelets.

Methods

Materials

CB (Association of Powder Process Industry and Engineering, Japan) and $C_{60}(OH)_{24}$ (Tokyo Progress Sysytem, Tokyo, Japan) were prepared as described previously[9] Fluoresbrite carboxylate microspheres (diameter, 6 μm) were obtained from Polysciences Inc (PA, USA).

Cell Culture

Mouse macrophages cell lines (RAW264.7) were obtained from Dainippon Sumitomo Phrma (Osaka, Japan) and were cultured in RPMI1640 with 10% (v/v) fetal bovine serum (Hyclone, Utah, USA). Cells were cultured in RPMI1640 with 2% (v/v) fetal bovine serum plus sonicated CB (0–100 μg/ml) or $C_{60}(OH)_{24}$. Cells were passaged every 3–4 days.

Lactate Dehydrogenase (LDH) Assay

LDH activity was analyzed with a CytoTox 96 non-radioactive cytotoxicity assay kit (Promega, Madison, USA) according to the manufacturer's protocols. RAW264.7 cells at 50–60% confluence were treated with CB or $C_{60}(OH)_{24}$ alone for 24 h, or 13 or 50 days. In addition, cells at 50–60% confluence were treated with CB or $C_{60}(OH)_{24}$ for 50 days or 8 days, respectively, and Ox-LDL was then added (Biomedical Technologies, MA, USA) (0–100 μg/ml) for a further 2 days. LDH activity in the culture medium was measured based on absorbance at 490 nm using a microplate reader (ARVO; PerkinElmer, Japan). Cytotoxicity was expressed relative to basal LDH release in untreated controls. Cells at 50–60% confluence were treated with $C_{60}(OH)_{24}$ for 8 days or 6-μm beads for 3 days, and Ox-LDL or Dil-Ac-LDL (Biomedical Technologies) was then added for 24 h. Cells were examined under a microscope (Zeiss Axiovert 25, Göttingen, Germany).

Proliferation Assay

Cell proliferation assay was carried out using a Cell Counting-8 kit (Dojindo Laboratories, Kumamoto, Japan) according to the manufacturer's protocols. Cells were cultured in 12-well plates, and were treated with Ox-LDL (100 μg/ml) for 5 days to induce foam cell-like formation, after which $C_{60}(OH)_{24}$ (0–100 ng/ml) was added to the cells for a further 2 days. Cell growth was measured based on absorbance at 450 nm as detected by the ARVO micro-plate reader.

Treated and untreated cells were fixed with 4% paraformaldehyde for 15 min at room temperature. After washing, cells were stained with filtered Oil Red O solution (60% isopropanol) or Giemsa solution for 0.5 h–2 h at room temperature. After washing, the cells were examined under a microscope (Olympus BX-51, Tokyo, Japan). The Dil-Ac-LDL incorporated macrophages were captured directly from an RGB camera attached to the microscope (Zeiss Axiovert 25, Göttingen, Germany) and displayed on a Adobe photoshop CS2 to quantify fluoro-intensity in macrophages.

Western Blotting of LOX-1 and SR-AI

Samples were obtained from RAW264.7 cells treated with lysis buffer (20 mmol/L Tris-HCl, pH 7.4, with 150 mmol/L NaCl, 1 mmol/L EDTA, 1 mmol/L EGTA, 2.5 mmol/L sodium pyrophosphate, 1 mmol/L β-glycerol phosphate, 1 mmol/L Na_3VO_4, 1 μg/ml leupeptin, 0.1% protease inhibitor cocktail (Nacarai Tesque, Kyoto, Japan), and 1% Triton X-100). Equal amounts of proteins (10 μg/ml) were subjected to reducing sodium dodecylsulfate–polyacrlamide gel (10%) electrophoresis electrophoresis after boiling with 1 mmol/L dithiothreithol and were transferred to nitrocellulose membranes (Pall Corporation, Ann Arbor, MI, USA). After blocking with 5% (w/v) skim-milk in T-TBS (10 mmol/L Tris-HCl, pH 7.5 with 10 mmol/L sodium chloride and 0.1% Tween 20) buffer, the membrane was incubated with primary antibody (R&D biosystems, MN, USA) (LOX-1; 1:100 dilution, scavenger receptor-type AI (SR-AI); 2 μg/ml) at 4°C overnight. After washing, the membrane was incubated with secondary antibody (anti-mouse horseradish peroxidase-conjugated antibody and anti-rat horseradish peroxidase-conjugated antibody, respectively; 1:5,000-10,000 dilution) at room temperature for 1 h. LOX-1, SR-AI and β-actin protein were visualized using the ECL system (Amersham Biosciences, Buckinghamshire, UK).

Pro-MMP-9 Secretion Assay

Culture medium was collected from cells treated with $C_{60}(OH)_{24}$ alone for 10 days or with $C_{60}(OH)_{24}$ for 8 days followed by 2 days of co-treatment with Ox-LDL (100 μg/ml). Pro-MMP-9 in culture medium was analyzed using a mouse pro-MMP-9 sandwich enzyme-linked immunosorbent assay kit (B&D systems, MN, USA) according to the manufacturer's protocols. Pro-MMP-9 in culture medium was detected by absorbance at 450 nm, and concentration was calculated using a standard curve.

Reverse Transcription (RT)-Polymerase Chain Reaction (PCR) for Tissue Factor mRNA Expression

Expression of tissue factor mRNA in cells treated with $C_{60}(OH)_{24}$ alone for 10 days or with $C_{60}(OH)_{24}$ for 8 days followed by 2 days with Ox-LDL (100 μg/ml) and were quantified by RT-PCR. Tissue factor primer sets were as follows: tissue factor; forward 5'-CGGGTGCAGGCATT CCAGAG-3' and reverse 5'-CTCCGTGGGACAGAGAG-GAC-3', glucose-3-phosphate dehydrogenase; forward 5'-ACCACAGTCCATGCCATCA-3' and reverse 5'-TCCAC CACCCTGTTGCTGTA-3'. The PCR products were electrophoresed on 2% agarose gels, and were stained with ethidium bromide, visualized using ultraviolet and recorded. Expression levels of tissue factor were adjusted against glucose-3-phosphate dehydrogenase expression levels.

Platelet Aggregation Assay

Whole blood was collected from the ear artery of male Japanese white rabbits (n=3; body weight, 3–5 kg) into tubes containing 3.8% (w/v) tri-sodium citrate, and were kept at room temperature for 5–10 min. After pre-treatment with or without CB (5 μg/ml) or $C_{60}(OH)_{24}$ (5 μg/ml) at room temperature for 5 min, ticlopydine hydrochloride (0–4 mmol/L) was added to whole blood, which was then left to stand at room temperature for a further 15 min. Adenosine diphosphate (ADP) (0–80 mmol/L) induced aggregation was analyzed using a whole blood filtration pressure aggregometer (WBA analyzer, Yokohama, Japan).[10] Reaction tubes containing 200 μl aliquots of whole blood were placed an incubation chamber at 37°C for 2 min, followed by addition of 22.2 μl of ADP. The pressure rate was standardized using a grading curve of 4 different ADP concentrations (0, 1, 2, 4, 8 mmol/L or 0, 10, 20, 40, 80 mmol/L, respectively) on the x-axis and pressure rate on the y-axis. The concentration of ADP causing an increase in pressure rate was calculated and was applied as the platelet aggregatory threshold index. Experiments were performed at least 3 times.

Statistical Analysis

Data are shown as means ± SD. Statistical evaluation was performed by ANOVA. Values of $p<0.05$ were considered statistically significant.

Results

Effects of CB on RAW264.7

The effects of chronic exposure to CB were examined by treating RAW264.7 cells with CB (0–100 μg/ml) for 24 h, 13 days and 50 days. We observed marked CB (100 μg/ml) uptake in RAW264.7 cells at days 13 and 50 (Figs 1B, d and C, d). However, cytotoxic morphological changes, such as cytosolic phagosome formation, cell disorientation and decreased cell density, were not observed (Figs 1A, B and C, a–d). No significant cytotoxic injury (based on LDH